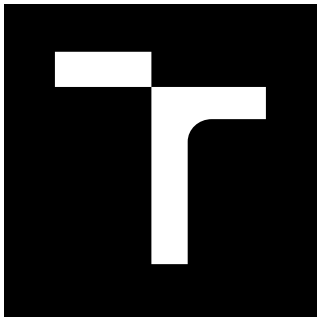


# BRNO UNIVERSITY OF TECHNOLOGY

VYSOKÉ UČENÍ TECHNICKÉ V BRNĚ

## FACULTY OF MECHANICAL ENGINEERING

FAKULTA STROJNÍHO INŽENÝRSTVÍ

## INSTITUTE OF MATERIALS SCIENCE AND ENGINEERING

ÚSTAV MATERIÁLOVÝCH VĚD A INŽENÝRSTVÍ


# PREPARATION OF CERAMIC-METAL COMPOSITES FOR BALLISTIC PROTECTION

PŘÍPRAVA KOMPOZITŮ KERAMIKA-KOV PRO BALISTICKOU OCHRANU

**BACHELOR'S THESIS**
BAKALÁŘSKÁ PRÁCE


**AUTHOR** — **Jakub Hladík**
AUTOR PRÁCE

**SUPERVISOR** — **doc. Ing. David Salamon, Ph.D.**
VEDOUCÍ PRÁCE



**BRNO 2019**

BRNO UNIVERSITY OF TECHNOLOGY
FACULTY OF MECHANICAL ENGINEERING

# Bachelor's Thesis Assignment

| | |
|---|---|
| Institut: | Institute of Materials Science and Engineering |
| Student: | **Jakub Hladík** |
| Degree programm: | Applied Sciences in Engineering |
| Branch: | Materials Engineering |
| Supervisor: | **doc. Ing. David Salamon, Ph.D.** |
| Academic year: | 2018/19 |

As provided for by the Act No. 111/98 Coll. on higher education institutions and the BUT Study and Examination Regulations, the director of the Institute hereby assigns the following topic of Bachelor's Thesis:

## Preparation of ceramic-metal composites for ballistic protection

**Brief description:**

Ballistic protection together with firing power and mobility are among the three basic components necessary for successful mission of military units. The development of weapons and military equipment must maintain a balance between these capabilities. A novel trend in development of ballistic protection is to minimize the weight to limits mobility restrictions, especially for combat vehicles. Therefore, there is a transition from metals with high density to composite materials with low density. The aim of this bachelor thesis, besides the literature review, is to prepare and subsequently characterize materials for ballistic protection.

**Bachelor's Thesis goals:**

1. A literature review of the research and applications in the field ceramic-metal composites for ballistic protection.
2. Experimentally prepare and characterize ceramic-metal composites.

**Recommended bibliography:**

DAVID, N. V., X. L. GAO and J. Q. ZHENG. Ballistic Resistant Body Armor: Contemporary and Prospective Materials and Related Protection Mechanisms. Appl. Mech. Rev. 62, 050802-050820, DOI: 10.1115/1.3124644, 2009.

ZORAN, Odanović and Biljana BOBIĆ. Ballistic protection efficiency of composite ceramics/metal armours, Scientific-Technical Review, vol. LIII, no. 3, 2003.

Students are required to submit the thesis within the deadlines stated in the schedule of the academic year 2018/19.

In Brno, 2. 11. 2018

VYSOKÉ UČENÍ TECHNICKÉ V BRNĚ FAKULTA STROJNÍHO INŽENÝRSTVÍ DĚKANÁT

L. S.

prof. Ing. Ivo Dlouhý, CSc.
Director of the Institute

doc. Ing. Jaroslav Katolický, Ph.D.
FME dean

# ABSTRACT

Aim of this bachelor thesis is fabrication of ceramic-metal composite for ballistic protection, the main focus is on the materials interface. Properties of used ceramic and metal materials are described as well as applicable mechanical tests. Alumina / aluminum composite was prepared experimentally by gravity casting/sintering of aluminium among the alumina hexagons. Various temperature conditions were tested to achieve the optimal casting conditions at the lowest possible temperature. Prepared composite was tested by a ballistic impact according to NIJ Standard-0108.01 and NATO Standard STANAG 2280. Properties of the aluminium/alumina interface were verified by the fracture analysis of damaged samples and by a special version of four-point beam bending test. Also, a brief examination of aluminium microstructure was made.

# KEYWORDS

Adhesion, alumina, aluminium, ceramic-metal composite, ballistic defence, slip casting, gravity casting

# ABSTRAKT

Cílem této práce je příprava keramicko-kovového kompozitu pro balistickou ochranu. Přičemž velká pozornost se klade na rozhraní obou materiálů. Práce popisuje jak vlastnosti používaných keramik a kovů, tak i aplikovatelné mechanické testy Kompozit na bázi oxidu hlinitého a hliníků byl experimentálně připraven metodou gravitačního lití / slinování hliníků, která vedla ke spojení s korundovými hexagony. K dosažení optimálního výsledku a co nejnižší teplotě lití bylo třeba vyzkoušet několik teplotních režimů. Připravené vzorky byly balisticky testovány na základě norem NIJ Standard-0108.01 a NATO Standard STANAG 2280. Vlastnosti rozhraní byly ověřeny pomocí lomové analýzy vzorků, která zkoumala vzorky poškozené balistickým testováním. Za účelem zkoumání rozhraní byla připraveny speciální zkouška čtyřbodým ohybem. Dále bylo provedeno předběžné zkoumání mikrostruktury hliníku.

# KLÍČOVÁ SLOVA

adheze, korund, hliník, keramicko-kovový kompozit, balistická ochrana, slip casting, gravitační lití

# ROZŠÍŘENÝ ABSTRAKT

Bojeschopnost moderních jednotek lze posuzovat třemi základními parametry: palebná síla, pohyblivost jednotek a balistická ochrana. Každá z těchto vlastností má svůj nezastupitelný význam. Tyto potřeby jsou však často protichůdné a nelze je všechny stoprocentně uspokojit. Závažný problém činí požadavek vysoké mobility a balistické ochrany [1].

Ověřeným prostředkem v balistické ochraně je homogenní za studena válcovaný pancíř. Tento pancíř má pro tento účel výborné vlastnosti. Jeho nevýhodou je však relativně vysoká hmotnost. S výskytem silnějších ráží a průbojných střel, získává tato nevýhoda na významu. Částečně jí lze kompenzovat navýšenou kapacitou motoru a posílením pohonné jednotky. U některých typů bojových vozidel se uvažuje letecká přeprava nebo obojživelnost, a proto nemohou sami mnoho vážit. V této situaci pro zachování balistické ochrany není jiné cesty než využití nových přístupů [2].

Jedním z těchto přístupů je využití již zmiňovaného kompozitu. Nárazovou plochu tvoří keramiky. Jejich funkce lze v angličtině vyjádřit třemi „dé“ (decelerate, deform and distribute), tedy zpomalit a zdeformovat střelu a rozptýlit energii do větší plochy. Aby mohla tento úkol plnit i v případě průbojných střel s kalným nebo wolframovým jádrem, musí být keramika velice tvrdá [3].

Po dopadu střely je část kinetické energie střely spotřebována na tvorbu nových povrchů a keramiky se tříští. Urychlené střepiny jsou pro posádku obrněného vozidla stejně nebezpečné, jako zbytky projektilu, proto na řadu přichází záchytná vrstva kovu. Ten na rozdíl od keramiky musí být houževnatý, aby dokázal střepiny a projektil udržet [3].

Běžně se kompozity připravují sendvičovou metodou, kdy se jednotlivé vrstvy skládají na sebe a lepí pomocí pryskyřic. Jako lepidla se mohou používat flexibilní pryže na bázi polyurethanu, které kromě soudržnosti materiálu fungují částečně i jako tlumič a snižují poškození keramiky. Přesto, že jsou v dnešní době tyto lepidla velice kvalitní, musí být dopadová plocha kompozitu překryta polymerem, který brání vypadávání keramiky ze štítu v blízkosti zásahu. Pryskyřice mají omezenou životnost v rámci několika let a po této době je nutné bezpečnostní prvek vyměnit, protože ztrácí své vlastnosti. Další Nevýhodou polymerů je jejich náchylnost k degradaci vlastností při vysokých teplotách [4].

Síla rozhraní mezi keramikou a podpůrným materiálem hraje velikou roli. Správná vazby je důležitá nejen z důvodu udržení keramiky na svém místě, ale zároveň ji i chrání před poškozením. Při střetu kompozitu s projektilem vzniká na povrchu štítu tlaková vlna. Pokud je vazba mezi materiály pro mechanickou vlnu neprostupná, z důvodu existence trhliny na rozhraní či příliš rozdílné impedanci užitých materiálů, dochází ke zpětnému odrazu vlny od rozhraní. Nekvalitní rozhraní vede k minimálnímu rozložení napětí uvnitř kompozitu a k přílišnému namáhání keramiky [5].

Proto se tato bakalářská práce zabývá přípravou kompozitu jinou metodou, a to zaléváním korundu hliníkem. Takto získaný kompozit má disponovat nejen dlouho životností (v rámci desítek let) ale snad i větší odolností proti opakovaným zásahům díky lepší fixaci keramiky ve štítu a pravděpodobně i lepší odolnosti rozhraní proti šíření trhlin.

V první, rešeršní části, se práce zaměřuje na princip funkce kompozitu, na způsoby přípravy materiálů, vlivy, které ovlivňují kvalitu štítu a způsoby testování kompozitu. Podrobněji se teoretická část zbývá materiály, které se v praxi používají a jejími vlastnostmi. Důkladněji je také zmíněna problematika testování kompozitů.

Praktická část popisuje metodu výroby kompozitu pro balistickou ochranu. Za tímto účelem byly využity keramiky ve tvaru osmistěnného hranolu s pravidelnou šestiúhelníkovou podstavou a výšce 12 a 16 mm. Korundová keramika byla připravena na ústavu Ceitec (CEITEC – středoevropský technologický institut, Brno, Česká republika) formovací metodou suspenzního lití nebo jednoosým lisováním a prošla následným vysokoteplotním slinováním při 1 550 °C. Keramiky byly zality

konvenčním čistým hliníkem EN-AW 1050 (ALMS Brno, Czech Republic) s minimální čistotou 99,5 hm%.

Kompozit byl připraven metodou gravitačního lití, která však svým přístupem více připomíná slinování. Hliník totiž nebyl roztaven odděleně od formy a nebyl v pravém smyslu lit, ale nacházel se již ve formě spolu s keramikou.

Úkolem práce bylo nalézt vhodný tepelný teplotní režim pro zalévání hliníkem. Sledovala se zabíhavost hliníku při jednotlivých tepelných režimech a výskyt slévárenských vad. Dále byly kompozity testovány balistickou zkouškou na základě norem STANAG 2280 a NIJ Standard-0108.01.

Důležitým parametrem při volbě teploty byla energetická efektivita procesu, proto byla snaha teploty snižovat. Prodleva na teplotě zůstávala stejná a trvala 30 min. Z původních 900 °C byla teplota snížena na 800 °C a následně na 720 °C. Výsledná kvalita odlitků byla podobná. Až při odlévání kompozitu při 680 °C došlo k nedostatečnému zatečení hliníku. Důvodem byla existence oxidických plen a nedostatečného času pro tečení.

Pro ověření vlastnosti rozhraní mezi hliníkem a keramikou byly připravovány vzorky pro mechanické testování speciální verzi čtyřbodého ohýbu. Tato zkouška slouží pro měření adhezní práce nutné pro oddělení hliníku od keramiky.

Dále byla provedena analýza lomových ploch kompozitů po balistické zkoušce a strukturní analýza hliníku po odlití.

Výsledek balistické zkoušky ukázal, že kompozit obsahující keramiku o tloušťce 12 mm odolává kinetickým hrozbám stupně III. dle normy NIJ 0108.01 což odpovídá průbojné ráži 7,62 mm x 53 mm (puška Dragunov). Druhý typ kompozitu obsahující korundovou keramiku o tloušťce 16 mm splňuje standard STANAG 2280 stupeň A4. Konkrétně byl tento štít vystaven průbojné ráži 12,7 mm x 108 mm.

Analýza lomové plochy ukázala relativně dobrou odolnost rozhraní korund-hliník proti šíření trhlin.

Strukturní analýza hliníku za pomoci elektronové a optické mikroskopie odhalila výskyt dendritické struktury uvnitř materiálu a neočekávaně velké množství intermetalických fází. Byla také zjištěná výrazná heterogenita ve velikosti zrn, která byla zdůvodněna teplotním gradientem mezi dnem a vrchem formy.

Zkouška čtyřbodým ohybem neposkytla takové výsledky, jaké byly očekávány. Během zkoušení se nepodařilo detekovat délku trhliny šířící se po rozhraní a podařilo se získat jen údaje o odporu vzoru proti namáhání ohybem. Tyto informace zahrnovaly, jak vliv šíření trhliny, tak i vliv zpevnění materiálu. Získané hodnoty byly zaneseny do grafu se závislostí napětí v ohybu na průhybu a byly vzájemně porovnávány.

Hodnoty naměřené pro vzorky, vyrobené při stejné teplotě, projevovali na počátku podobný průběh. K výraznému poklesu odporu však docházelo dříve u vzorků s nižší délkou prodlevy a vyšším hodnotou teplotního přestupu mezi formou a pecí.

Od ostatních se výrazně lišil vzorek připravený při teplotě 800 °C. Ten činil nejnižší odpor vůči ohybu. Zkouška u něj vedla téměř k úplnému porušení vzorku. Šířením trhliny neprobíhalo po rozhraní, ale skrze vrstvu hliníku. Toto a dále viditelný výskyt trhlin na povrchu hliníku dalších vzorků vedl k podezření, že trhliny se nešířily po rozhraní, ale materiálem hliníku.

Důvodem proč experiment nevyšel, tak jak by měl by mohla být nedostatečná kvalita vzorku. Především pak nedostatečně ostře připravená trhlina a geometrie. Je také pravděpodobné, že odolnost rozhraní proti šíření trhlin byla natolik vysoká, že převyšovala odolnost hliníku. V tomto případě by adhezní práci po rozhraní nebylo možné tímto testem měřit.

S ohledem na dosažené výsledky lze teplotu 720 °C považovat za vhodnou pro přípravu daného kompozitu. Důležitou se ukázala potřeba dostatečné doby prodlevy na teplotě a vhodná úprava přestupu tepla mezi formou a pecí. Přestup tepla lze upravovat vhodnou izolací. Potřeba regulace je spojena s absencí vtokové soustavy a s rizikem výskytu staženin.

Překvapivý výsledek ukázaly strukturní analýza litého hliníku. Ačkoli původní hliník měl vysokou čistotu 99,5 hm% objevilo se ve struktuře velké množství fází. Vznik eutektik byl pravděpodobně zapříčiněn mikro-segregací prvků, které se do materiálu dostaly během výroby odlitku. Přesný charakter intermetalik není znám a bude v blízké budoucnosti předmětem výzkumu. V současné chvíli se odhaduje, že by se mohlo jednat o oxidy.

HLADÍK, Jakub. *Příprava kompozitů keramika-kov pro balistickou ochranu.* Brno, 2019. Dostupné také z: https://www.vutbr.cz/studenti/zav-prace/detail/117585. Bakalářská práce. Vysoké učení technické v Brně, Fakulta strojního inženýrství, Ústav materiálových věd a inženýrství. Vedoucí práce David Salamon.

# DECLARATION

I declare that this bachelor´s thesis Preparation of ceramic-metal composites for ballistic protection was worked out on my own using literature which I cited according to the rules.

In Brno on the: _____ _____

Jakub Hladík

# ACKNOWLEDGEMENTS

I would like to thank to my supervisor doc. David Salamon, Ph.D. for his valuable advises, supervision, friendly approach, kindness and patience in checking this thesis. Furthermore, I would like to thank to all workers in a research group of advanced ceramic materials in CEITEC who were always willing to help. Least but not last, I would like to thank to Ing. Zdeněk Chlup, Ph.D. worker of the Czech Academy of Science for his advises and help in mechanical testing.

# CONTENT

# 1 INTRODUCTION

The readiness of a modern combat units can be evaluated according these fundamental factors: firepower, mobility and ballistic defence. All of them are important and they cannot be neglected. However, all these requirements cannot be fulfilled completely at once. Most crucial is the problem how to insecure the protection against deadly threats without loose of mobility [1].

The rolled homogenous armour steel (RHA) is a one of the defensive materials. This armour combinates the excellent mechanical properties (hardness and toughness), a high affordability and compatibility with the vehicle bodywork. On the other hand, it has relatively high mass. This disadvantage is even more serious with an occurrence of high energy armour piercing threats. The problem can be compensated by an increase of engine power and by reinforcement of motion gears of the armoured fighting vehicle (AFV). However, the light armoured vehicles (LAV) often requires the possibility to be transported by air. Also, the amphibious vehicle cannot weight much. Hence there is a need for a different approach [2].

The use of ceramic-metal composition is the one of such unconventional options. The mayor advantage of the composite armour is its light weight compared to full metal sheets. Ballistic equivalent has two times lower mass density compare to homogenous iron armour sheet in case of alumina aluminium composite. Benefits of composition came from the combination of the hard ceramic, which has ability to absorb a significant amount of energy, and a metal with a high toughness [1, 3].

Ceramics are consisted of ionic or covalent bonds, which are very strong. Ceramics are naturally very hard and have a high compression strength. That gives them a chance to deform the projectile. Sometimes if the ceramic hardness is high enough it can also make it to shatter. Then fragments should be intercepted by metal rear face more easily. Ceramics have also a low weight, compared to conventional steel plates [3].

On the other hand, ceramics are brittle. That makes them quite vulnerable to be damaged even by a less lethal impulse. Causing that the penetration resistance is considerately weakened in vicinity of impact. Even though the compression strength of ceramics is high their tension strength is weaker. That is the reason why the ceramic face needs to be combined with a metal [1, 6].

Ceramic-metal composite is more effective against the armour piercing and ammunition with a high velocity [6].

# 2 THEORETHICAL PART

## 2.1 Fabrication methods of ceramics

### 2.1.1 Forming methods

There is a several methods how to transform the ceramic powder into the compact shape. Some of them are dry methods, that means that no or only a small amount of binder have been used. Dry methods are generally used for more simple shapes, which is formed by forcing. Other techniques pour the powder which is dispersed in liquid [9].

The presence of the binder is often important in a forming mixture or a slurry. The Binder accts as a plasticiser in some forming methods such as extrusion or in case of injection moulding process. It also provides the manipulation strength of the greenbody. The possibility of a safety elimination of is another important requirement for binder. Polymers are popularly applicated because they undergo a degradation process during the high temperature so they can be removed from compact more easily [9].

Polyvinyl alcohol (PVA) and polyethylene glycol (PEG) are two commonly used polymers which are used as a binder [9].

#### Uniaxial pressing

Uniaxial pressing is one of the dry forming methods. Ceramic powder and a small amount of binder is poured into the form. As the name said, the powder undergoes the uniaxial pressure. The magnitude of pressure depends on the required relative density and on particle's distribution. To low size of particles size cause problems during the pressing. The ideal powder particles distribution is between 20 and 200 μm [9].

The advantage of this method is it low acquisition price, low operation cost and a high productivity when the automatization of process is applied [9].

On the other hand, only simple shapes can be made by uniaxial pressing. The uniaxial pressing is unsuitable for a preparation of a long components because of the friction between powder and a die [9].

#### Slip casting

Slip casting is one of the wet shaping methods. Suspension with content of ceramic powder and binder is poured in to a porous mold. The liquid contained in the suspension is absorbed by the porous material due to a capillary compression. The suspension hardens primary in vicinity of mold. The molds are typically made of plaster of Paris with some additives because of its affordability and good sucking properties [8, 9].

Slip casting can be used for preparation of full profiles as well as for casting of hollow objects. This method can be applied for manufacturing more complex shapes. The disadvantage is low productivity of this method, since the time needed for hardening the suspension is long [9].

### Gel casting

This method is suitable for preparation of a complex shapes. Manipulation strength is caused by polymerized monomers, which were present inside the liquid. The polymers form a net that keeps the powder particles on place. In the following thermal process polymers are degraded and then removed completely from the body of cast [7].

## 2.1.2 Sintering methods

### Hot uniaxial pressing

Unlike to the forming version of uniaxial pressing this method use a high temperature which makes the powder sinter. This method produces high-density components without need of a high-quality powder. The pressure has a positive effect on the sintering process so it can be performed by a lower temperature (approximately the half of the melting point). Decrease of temperature leads reduces the growth of grains. This method can be used to densify the covalent ceramics such as $B_4C$ or SiC without need of additives [9].

The disadvantage of hot uniaxial pressing is its low productivity, importance of expensive dies and a shape limits of the components. Dies usually have a low lifetime due to existence of high temperature. Usually it cannot be made of metals because the densification temperatures are still too high, so they may become ductile. Dies are generally made of graphite which is inexpensive and can be machined easily. However, this material is unsuitable for some applications because of its reactivity [9].

The hot uniaxial pressing is not commonly used by plants because of the low productivity but it is frequently used in laboratories and in research centres [9].

### High temperature sintering

The greenbody prepared by any shaping methods are subjected to a high temperature. The sintering process is driven by the decrease of the Gibbs free energy which is caused by decrease of surfaces. The advantage of this method is its simplicity and a low cost. Unlike to hot uniaxial pressing this process does not require an expensive form.

A disadvantage of the method is the high temperature and relatively long dwell time. That leads to a bigger grain size and a decrease in mechanical properties. There is also a risk of deformation of components because of the compression during sintering [9].

On the other hand, a large mass of ceramic is used for a whole defensive structure of AFV. Despite the importance of a high properties of armour, higher expenses dissuade from application of more advanced sintering methods.

## 2.2 Fabrication methods of metals

### Strain hardened plates

Cold rolled metals plates are frequently used for the preparation of the armour. The ceramic is glued to the surface of plate by high strength adhesives. Epoxide resins are commonly used in ballistic for this task.

The expiration time of epoxides is low, and it can be counted in years. After that time armour must be changed. Resins are also vulnerable to a high and low temperatures [1].

### Extrusion

Another option are the extruded profiles filled by the prisms made of ceramics. Metals and alloys with a low melting point can be extruded. Hollow with rectangular or triangular spacing are fabricated by this method. Ceramic prisms are inserted into spaces inside the metal. The position of the ceramic can be ensured by an annealing. . The expiration time depends on the oxidation resistance of metal because there is no need for adhesives [10].

### Die casting

Manufacturing process usual for producing of non-iron alloys such as aluminium, copper, magnesium or zinc materials. The advantage of this process is a high quality of surface of the cast and a high productivity rate. Die casting is very popular technology in automotive where a cost-effectivity and sustainability is needed [11].

On the other hand, die casting demand inconsiderable expenses. Besides the die cast machine an expensive metal form is needed. These forms provide a low cycling times because the material has a high degree of conductivity. High cooling rate is however dangerous for ceramics [11].

### Gravity casting

Gravity casting is relatively cheap method. Depending on the current technology, there is not high demand to the quality of a form compared the case of die casting. The quality of the surface is generally low and there is often request for an additional working.

In the experimental part of this thesis, modification of gravity casting of aluminium was used. This process is quite unusual for the casting of aluminium. Which is generally processed by different methods for example by the die casting. The problem makes the low casting fluidability of aluminium. The current method was in many ways more like a sintering process the to the gravity casting. The aluminium was melted in the form instead of being melted in the casting ladle.

## 2.3 Performance aspects

### 2.3.1 Fracture mechanism

Kinetic energy of the projectile may cause its deformation or even the destruction if the dynamic strength is excited. At this stage the hardness difference is important. If the plate is soft compared to projectile, it is likely, that the stress induced inside of projectile will not reach the level causing the fragmentation. Obviously, the risk of support plate to be penetrated is greater [10].

Microfractures start to excite under the impactor just a few minutes after the impact. The plastic behaviour of ceramic is almost none-existing because of the lack of slip systems in its matrix and high porosity of material. Besides, the time scale of the process is estimated to several milli seconds so plastic response is limited even in case of conventional ductile materials [10].

The impact generates a stress waves which travel through the volume of the plate since they are reflected by a rear surface of the tile. High energy of these waves rises to hoop tensile stress which leads to formation of radial cracks. As the tile is bending under the force of impact, radial cracks are running from the back face toward the front face of the plate. Radial cracks disrupt cohesiveness of the material. The conoid crack zone appears when the density of cracks grows up enough. After that fractures no longer keep together, and they are accelerated by the rest of kinetic energy towards the support plate [10].

The shape of conoid can be diverse according to shape and construction of the projectile and the facing plate. The stand of the conoid can be also limited by the borders of tile. Although previous studies [10 – [27-30]] shown that for alumina the angle of the surface of conoid is usually 65° [10].

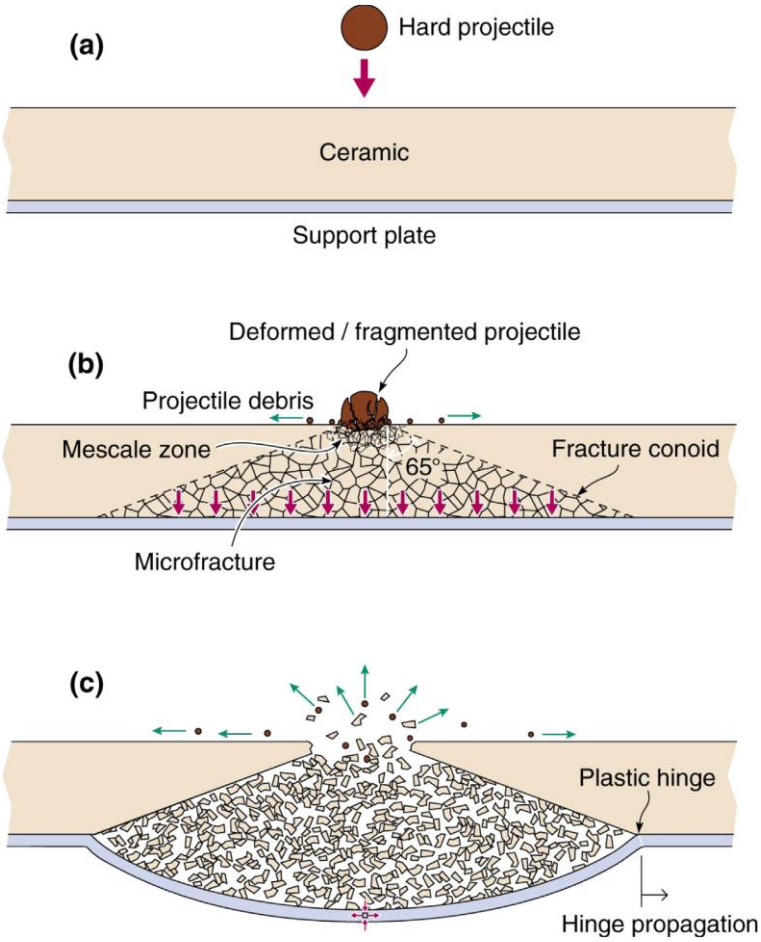


*Picture 1: A schematic illustration of the penetration mechanisms of a supported ceramic impacted by a hard metal sphere at zero obliquity. A second impact whose fracture conoid intersects the first more easily penetrates the composite panel [10]*

### 2.3.2 Materials

#### *2.3.2.1 Ceramics*

Structural ceramic for use as ballistic defence was first developed by US during 1960$^{th}$. Primary it was designed as body armour and a protection inside helicopter seats. It was important to find the lightweight alternative of metal armour. The sufficiency of this design was proved and ceramic materials such as zirconia and alumina started to be used in the ballistic defence [12].

Ceramics differs in the mechanism how it absorbs the kinetic energy compare to the metals. Metals primary absorbs the energy through the plastic deformation however the ceramics dissipate the energy through the fracture mechanism. The energy is factually "spent" by creating of micro cracks and new surfaces in the matrix. That obviously lead to a destruction of the ceramic protective structure. Formation of the large number of fragments from the original material is more desired rather than the development of the larger cracks [12].

The fracture mechanism is so complex that the material performance cannot be estimated by just mentioning the single one property. *The ability of ceramics to provide ballistic protection depends on both physical and mechanical properties such as density, porosity, hardness, fracture toughness, elastic modulus, sonic velocity (velocity of sound in the ceramic), and mechanical strength*[12] [12].

Ceramic material can be divided into groups according to its chemical aspect and weight density. $Al_2O_3$ and $ZrO_2$ represent the typical oxygen-based ceramics. Non-oxide ceramics are more advantageous and adequate for use as light weight armour because of theirs excellent mechanical properties and (except some examples) low weight. However, they are manufactured by hot pressing which affects their price [12, 13].

| | | Fine ceramics | | | Metals | | | | |
|---|---|---|---|---|---|---|---|---|---|
| | | Alumina | Silicon carbide | | Aluminium | | Steel | | Titanium |
| | | $Al_2O_3$: 99.8% | SiC | | EN AW 1050-O | EN AW-5083 | Armox 500T | Secure 500 | Ti-6Al-4V |
| Density | [g/cm3] | 3.9 and above | 3.1 | | 2.7 | 2.66 | 7.9 | 7.85 | 4.4 |
| Hardness (HV) | [GPa] | 16 | 24 | (HBW) | 20 | 75 | 480 - 540 | 480 - 530 | 332 |
| Yield strength | [MPa] | - | - | | 20 min | 110 | 1250 | 1300 | 827 |
| Tensile strength | [MPa] | 248[f] | 129[g] | | 60 - 95 | 270 | 1,450 – 1,750 | 1,600 | 896 |
| Compressive strength | [MPa] | 2350 | 1,395[a] | | | | | | |
| Fracture toughness | [M*Pa*$m^{1/2}$] | 4 | 3 | | | | | | |
| Young's modulus | [GPa] | 390 | 410 | | 69 | 71 | 210 | 210 | 114 |
| Poisson's ratio | [-] | 24 – 26[c] | 0.16 | | 0.33 | 0.33 | 0.33 | 0.33 | 0.33 |
| Impact energy | [J] | - | - | | | | 32.00 | 25 | 22-27[b] |
| Thermal shock resistance (ΔT) | [°C] | 200 | 450 | | | | | | |
| Elongance | [%] | 0 | 0 | | 25 | 12 | 8 | 9 | 14 |
| Solidus temperature | [°C] | 2,042[c] | 2,600[d] | | 646 - 657 | 575-638 | ~1,440[e] | ~1,440[e] | 1,668 |
| Literature: | | [14] | [14] | | [18] | [19] | [20] | [21] | [23] |

a) Original literature: [15]
b) Original literature: [29]
c) Original literature: [24]
d) Original literature: [16]
e) Original literature: [17]
f) Original literature: [22]
g) Original literature: [42]

*Table 1: Comparison of selected properties of ceramics and metals*

#### 2.3.2.1.1 Alumina

Aluminium oxide also known as corundum is well known for its chemical and mechanical properties across technical branches. Corundum is often used as a refractory insulation because of its thermal and chemical stability. It is also used in ballistic according to its low price and good mechanical properties. The density of the alumina is higher amongst ceramics (3.95 $g \cdot cm^{-3}$). Unlike to non-oxide ceramic the hot pressing is not needed, so the manufacturing process is more "affordable" and productive. Nevertheless, the use of hot press offers an increase of mechanical properties [13, 24].

Aluminium oxide is an allotropic material, but the most common and thermodynamically stable form is α phase (hcp). The stochiometric can radically change when the impurities are present in the crystal lattice [24].

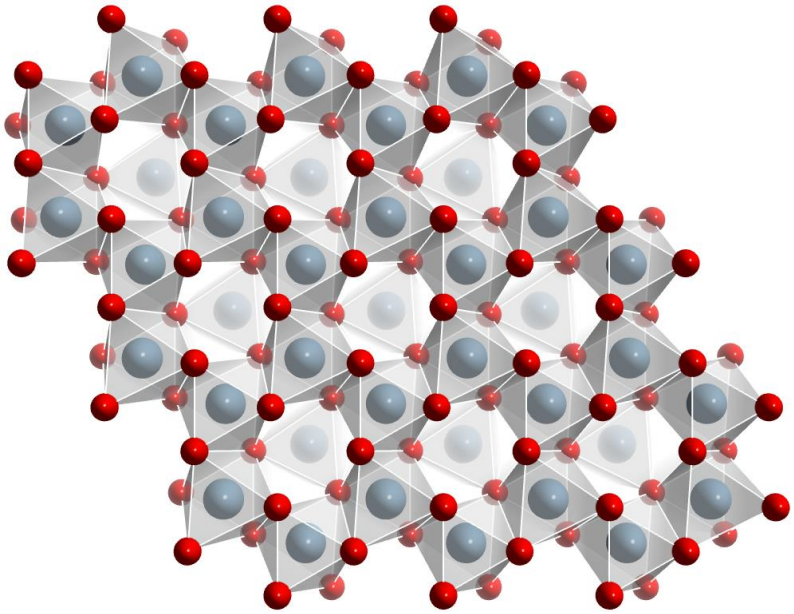

*Picture 2: Crystal structure of the parent structure of ruby, alpha lattice [25]*

High ionic bound between aluminium and oxygen ions has caused that the melt temperature is high (approximately 2,040 °C, Table 1). The preparation of $Al_2O_3$ by melting would be extremely expensive and exacting. Alumina is often manufactured by a sintering process at a high temperature. Typically, ceramic is sintered on the temperature between 1,300 and 1,500 °C. The final properties of alumina depend on the purity of incoming powder and the sintering level and grainsize [3, 24].

### *2.3.2.2 Metals*

**Al alloys**

Rolled homogenous steel can be replaced by an aluminium. More than that the aluminium shield can perform even better in some conditions. First existence of the aluminium armour appeared in 1954, when a carrier M113 was introduced by an American army. Design of the carrier was focused on elimination of transporters weight of to a minimum. The vehicle was able to withstand only a small firearm, but its speed and manoeuvrability was higher. Besides it was possible to transport the carrier by air [26].

Depends on the alloying elements the weight density of aluminium is around 2.7 gram per centimetre cubic. The weight density of rolled steel is almost three times higher. However, that does not necessarily mean that the aluminium equivalent of rolled steel armour is lighter. Easiest way how to compare ballistic materials is to define the required mass of material which can protect defined area against defined threat. Areal density is then counted for each kinetic threat. This areal density is not constant,

and it vary according to a calibre and velocity. Basically, areal density of both materials can be rated if the materials were subjected to same conditions during testing. According to The Army Research Laboratory [26] aluminium armour performed better than steel when they were subjected to a multiple shot [26].

One of the most commonly used wrought aluminium alloys is 5083 – H131 (see Table 1). It is magnesium 4.5 wt%, chromium 0.12 wt%, manganese 0.7 wt% alloy. 5083 is typically used after cold rolling which increase its hardness and yield strength. According to its chemical composition it cannot be heat treated. 5083 has a very good corrosion resistance. It is also weldable by the all method typical for aluminium alloys such as MIG or WIG [27].

Other wrought aluminium materials which are often used in ballistics are 7032-T64 and Keikor 2139.

**Ti alloys**

High strength, fracture toughness, crack propagation and excellent corrosion resistance makes titanium alloys a very interesting material. However, a high cost of titanium historically prevented from its use in ballistic defence of land troops and vehicles. For decades the main field of application was the aviation. Remarkably low density (4.5 $g \cdot cm^{-3}$) and high strength promised a noticeable decrease of operation costs in this industry. The availability of titanium changed in recent years. A new more economical technology has appeared. With an existence of a large competitive industrial base with a high level of forming and shaping technology, this factor let to increase of affordability of these materials [28, 29].

The Titanium becomes a relevant option in recent years when the conventional armours are being replaced by an expensive ceramic or composite one [29].

Titanium can exist in two kind of solid phases. The first one is an alpha phase which has a hcp crystal structure. In an unalloyed for of titanium this phase exists below the temperature of 882 °C. This phase has extremely low fracture toughness. Hence alloying elements are added to stabilize the beta and alfa phase. Depends to final phase composition three basic titanium alloys are defined: Ti – α, Ti -α β, Ti – β. Alpha – Beta titanium (Ti64) alloys are used in ballistic because of their weldability [29].

Another advantage of titanium alloy is the fact, that they can be heat treated. More importantly the mechanical properties can be increased by thermomechanical working. The effect of quenching is not so strong in the scale of thickness however the thermomechanical rolling provides excellent and uniform mechanical properties [29].

**Steel**

Comparison with rolled homogenous armour steel (RHA) often appears in number of articles and web pages. The reason is simple. In many aspects RHA is still the most popular defensive material. The combination of high availability, low price and high mechanical properties foretold the steel to be used in cases where the large volume of material is needed. Besides the behaviour of such material is more predictable and the ballistic performance can be reproduced easily.

Example of steel commonly used for purpose of ballistic protection is Secure 500. Usually delivered in the heat-treated state (quenched and tempered), armour provides certain ballistic resistance against standardized threats.

Representative chemical composition of the steel Secure 500 can be seen below.

Second example of a ballistic steel is Armox 500T. Mechanical properties of these steels are similar Table 1 but the Armox 500T has a higher impact energy. On the other hand Secure has a slightly better strength characteristics.

Both materials have chemical composition differ by the thickness of plates. The reason is to achieve a better quality of heat treatment.

| thickness | C | Si | Mn | P | S | Cr | Mo | Ni | Al |
|---|---|---|---|---|---|---|---|---|---|
| ≤ 50 mm | ≤ 0.32 | ≤ 0.40 | ≤ 1.00 | ≤ 0.015 | ≤ 0.005 | ≤ 1.50 | ≤ 0.50 | ≤ 0.70 | ≤ 0.110 |
| > 50 mm | ≤ 0.32 | ≤ 0.40 | ≤ 0.50 | ≤ 0.015 | ≤ 0.005 | ≤ 1.50 | ≤ 0.60 | ≤ 3.70 | ≤ 0.050 |

*Table 2: Chemical composition of Secure 500 – Heat analysis wt%. [21]*

| thickness | C | Si | Mn | P | S | Cr | Mo | Ni | B |
|---|---|---|---|---|---|---|---|---|---|
| ≤ 70 mm | ≤ 0.32 | ≤ 0.4 | ≤ 1.2 | ≤ 0.01 | ≤ 0.003 | ≤ 1 | ≤ 0.7 | ≤ 1.8 | ≤ 0.005 |
| ≥ 70 mm | ≤ 0.32 | ≤ 0.4 | ≤ 1.2 | ≤ 0.01 | ≤ 0.003 | ≤ 1.5 | ≤ 0.7 | ≤ 3.5 | ≤ 0.005 |

*Table 3: Chemical composition of Armox 500T – Ladle analysis wt%, The steel may additionally contain Ti, Nb and B [20]*

### 2.3.3 Adhesion

The adhesive bound between ceramic and metal is not only because of keeping both materials together, but its function is also transferring the shock waves from the ceramic to the rear face of armour. The task is to reduce the damage which will ceramic suffer by the reflected shock waves. By this mechanism part of the energy of the shock wave is softened during the way through the metal [5].

Besides the propagation of the crack through the interface of rear face and ceramic might by crucial in case of multiple shot. The crack forms a barrier between ceramic and metal for the shock wave. Then the shock wave is completely reflected at the end of ceramic and has a greater destructive impact on it [5].

Several adhesive bounds mechanism exists. However only three of them are mentioned in the thesis. Interlocking and chemisorption mechanism is more expected in case of metal ceramic interaction. The physical absorption is common in the case of polymer adhesives [5].

#### Interlocking

This mechanism is based on the existence of irregularities and micro pores on the surface of substrate material. The requirement is that the substrate is wetted by the second material or adhesive. Another term is the viscosity of the adhesive which must be low enough. Otherwise the material has not time to enter the micro porosity [5].

#### Physical absorption

Physical absorption is an interaction of intermolecular forces between both materials. These bounds are for example Wan der Waals or hydrogen bounds). The substrate must be wetted by the adhesive / second material. It is important for the existence of a good contact. Unlike to the previous mechanism, physical absorption does not require the penetration of the adhesive into the substrate [5].

#### Chemisorption

In case of Chemisorption materials are bounded together by the interatomic bounds (covalent, ionic or metallic). Obviously, these bounds are radically stronger compared to physical absorption. That is the reason why the surface treatment takes place before adhesion. Change of chemistry of the surface sometimes lead in change of adhesion mechanism from physicalsorption to chemisorption [5].

## 2.4 Testing

### 2.4.1 Armour Performance Standards

Like in the other branches of engineering there is a need of standards for ballistic armour. Since there is not a universal protection suitable for every application we need to describe ballistic performance of every material properly.

**NIJ Standard-0108.01**

Armour specimens must fulfil terms in Appendix I. Table 8 to be accepted by the standard. Besides there are other rules which must be followed. Fair hit was determined by standard. The impact is considered as the fair hit when the angle between perpendicular to the surface and the bullet trajectory is smaller than 5°, impact is located from edge of specimen or prior hit is at least 5 cm also the velocity must be meet. It is obvious that we can proclaim the hit as fair, when the conditions happened to be more suitable for penetration because the velocity was exceeded or the impact was situated to close to the edging, but the specimen withstand. However still the hit cannot be accepted when the angle is greater than 5° [30].

More detailed information describing kinetic classes are shown in the Table 8 in Appendix I.

Depend on the armour type the test consist of handgun or testing barrel which is situated towards the target. The projectile velocity is estimated by triggering devices with are connected to chronometer. The witness plate is placed behind the support of the test specimen. The plate shall be made of aluminium alloy. After every shot the witness plate is examined, if the penetration has occurred [30].

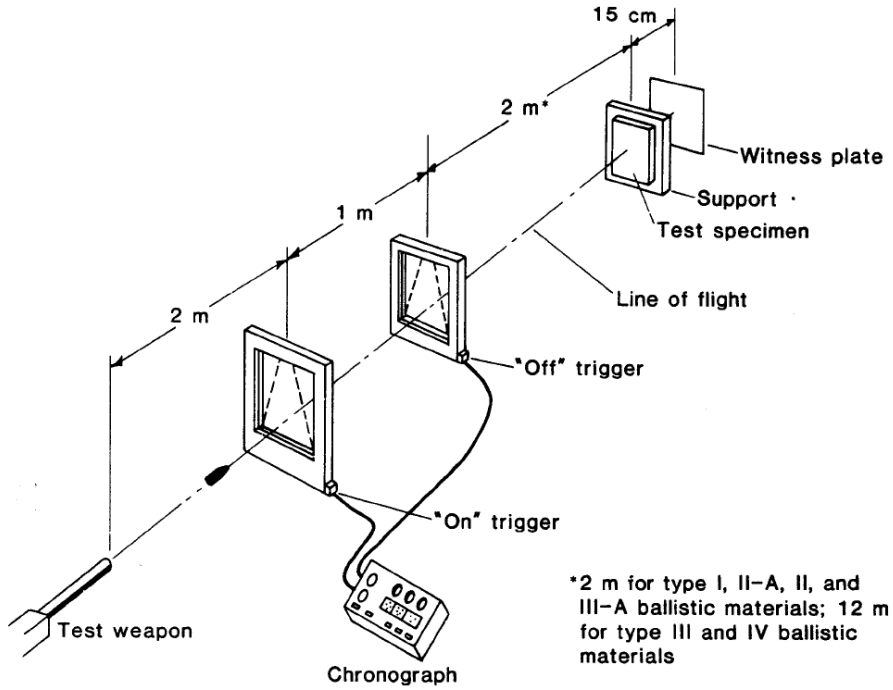


*Picture 3 - Ballistic test setup [30]*

### NATO AEP-55 STANAG 4569

Standardization Agreement – STANAG – was primary established for internal needs of North Atlantic Treaty Organization. However, the modified versions of standards are used in the other countries around the world. The full name of the NATO AEP-55 STANAG 4569 (volume 1) is: Protection Levels for Occupants of Logistic and Light Armoured Vehicles (LAV). Standard contains four annexes [31].

Annex A is focused on defining the bodywork with regard on protection against the threats caused by gunfire or artillery grenade explosion. The threats are separated in to five groups according to the Kinetic Energy (KE). Each performance level is represented by a typical kind of a weapon and specific ammunition. The whole categories are shown in the Appendix I. Table 9. Armour properties are expected to change in the surrounding of impact, so the multi-hit test is often required. Two pairs of impact are aimed into the single armour specimen. The first two shots are shot relatively close together. The maximal and minimal distance between the centre of impacts is defined. Another pair of shots is shot in the same manner, but they are placed in a longer distance from the previous two shots. The armour must withstand all these hits to fulfil the multi-hit requirement. Number and pattern of shots can diverse in case of a small target and a transparent armour [31].

Classes of kinetic threats are described in Table 9 Appendix I.

Both Annex B and C are designed for different type of threat. They are focused on Floor Protection Levels for Occupants for Grenade and Blast Mine Threats. The multi-shot testing is not required in case of defensive structure against blast threats [31].

### STANAG 2280

This standard was created for the evaluating of the ballistic resistance of building and temporary defensive structures such as Hesco Barrier Blast Wall. Nevertheless, the standard was used for the evaluation of ballistic composite. There is no significant difference in the procedure of testing compare to STANAG 4569 [32].

STANAG 2280 was the one of the standards used for evaluation of armour in the thesis. The standard 2280 dispones a wider scale of kinetic threats which have a sense to confront with the already mentioned composite. Used conditions (12.7 mm x 108 API B32, $V_{200}$ = 800 $m \cdot s^{-1}$, m 48g) were obtained by combining the kinetic requirements in class A4.

For more information about kinetic threats, see Appendix I. Table 10.

2.4.2 Mechanical adhesion tests

**Peel test**

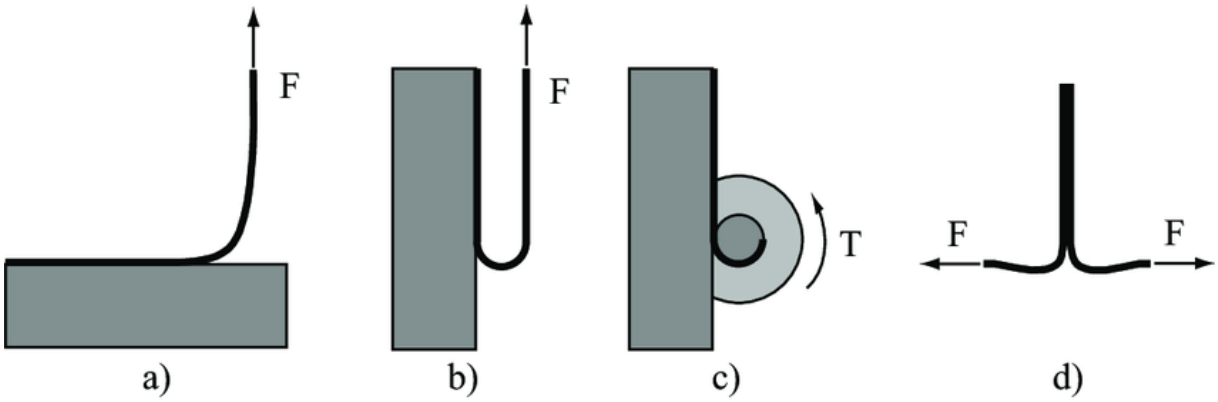


*Picture 4: 1: Four standard peel test configurations: (a) 90° peel test, the most commonly used configuration; (b) 180° test preferred when available space precludes the 90° test; (c) climbing drum or peel roller test, which has the advantage of controlling the radius of curvature of the peel strip; (d) T-peel test, preferred when testing adhesion of two flexible strips [33] (originally from [34])*

As the name says, a film of flexible material is peeled off the other. During this strength of an adhesive bound is measured. By this method, serious data about adhesive and cohesive force are earned. The output from this test is a graph which shows as the force vs the deflection. Hence the test does not only say how difficult is to peel out one material from another, but also other characteristics can be earned. One of these characteristics is fracture toughness [5].

There are various options how to perform the peel test. In some cases, a single force is applied to peel the flexible material off. Then we are talking about fixed arm test Picture 4 a), b). Both fixed arm and not fixed arm variants can differ by the angle. The fixed arm test can be performed at range of angles around 45 to 180 ° [5].

Each method suits to a different combination of material. T test Picture 4 d) is suitable for two flexible materials. However, it unsuitable for rigid to rigid bounding, then the application of floating roller Picture 4 d) is more appropriate [5].

Despite to the high informative qualities of such test it was not used for the task of the thesis. A low yield strength of aluminium would lead to a rupture of the film if it is too thin. The thick layer of aluminium would probably cause a complication of the test preparation. Also, the problem with low hardness of metal would lead to its release from the clamp jaw of the testing machine. Another problem is linked to a ceramic which is extremely hard. The problem is how to fix it without damage of machine components [5].

**Scratch test**

The scratch test uses a diamond stylus which is dragged across the surface of the film. Vertical load is controlled during the test and it is increased gradually [5].

For the task of evaluation critical value of vertical load is important. $P_{cr}$ says the minimum force which leads to a decomposition. After that clear channel appears in the film in places where the upper material is striped from the substrate. An existence of delamination can be checked by microscopy but more

$$P_{cr} = \frac{\pi r^2}{2}\left(\frac{2EW_{A.P}}{h}\right)$$

easily it can be noticed by a worker's sense of hearing. Since the delamination is followed by a characteristic acoustic emission [5].

The output of the test is a practical work which is needed for decomposition. Work could be count by using the previous equation. Where the "r" represents a contact radius of the indenter, "h" is the thickness of the film and "E" is the energy of adhesion. Analyse is complicated since the many proportions of the test must be known. To obtain regular value of adhesion energy we must know material properties of both materials, sharpness of the stylus and scratch elastic test distribution [5].

On the other hand, preparation of the test specimen is quite easy. Only the constant thickness and smoothness of the layer and a surface must be fulfilled. Test is quite universal from a sight of the adhesion energy. It can be used for a weak bound as well as the stronger bound [5].

This test however was not chosen for the need of thesis. The method was designed for the task of a thin film. Although in the real composite high volume of aluminium was used. Prepared specimen for the scratch test would probably slightly diverse by its chemical composition and thermal history [5].

**M**odified four-point beam bending test

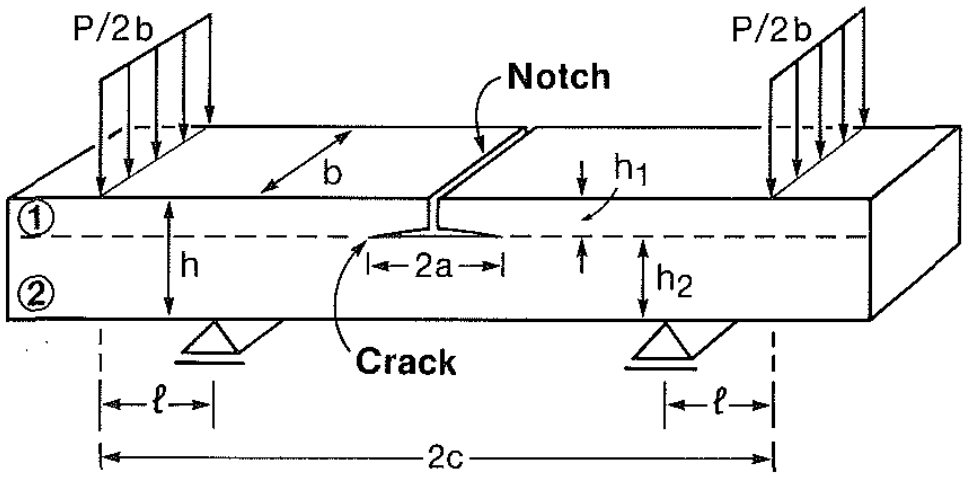


*Picture 5: A bimaterial, notched tour-point bending specimen with symmetrical interfacial cracks [35]*

Test specimen is consisted of two plates from bounded materials. The upper plate must be cut to prepare the notch in the middle without it bending process would behave as the nonmodified four-point beam bending test. Adhesion zone is weakened under the notch by the pre-crack. Crack can be prepared by an altering cycle of bending load or by local eliminating of the adhesion bound. In the experiment bound was removed by covering of the ceramic with graphite paper [35, 37].

Specimen for the task of 4PBT is quite difficult to prepare as it was claimed in [36] and will be approved in the experimental part in this thesis. On the other hand, specimen preparation can be prepared at conditions which fully represents the real one. Also, the mixed mode of the load caused by bending is in many similar to a fracture mechanism during the ballistic testing (as far as it can be compared) [36].

Four-point beam bending test (in the following text 4PBT) is an unusual way how to measure adhesive characteristic. The test is used in electrotechnology more frequently in the context of high temper-electrodes. But it can by also used in the larger scale. One of the examples is study N. Suansuwan, M. V. Swain [37] where this method was successfully used for measuring the adhesion energy between titanium and porcelain [36, 37].

# 3 EXPERIMENTAL PART

## 3.1 Preparation of Al2O3/Al composites

### Alumina preparation

Slip casted or uniaxially pressed alumina were used for the ballistic shields. The relative density of the casted alumina was approximately 98 %. The relative density of the pressed alumina hexagons was about 95 %. Both ceramics were manufactured in Ceitec institute (CEITEC – Central European Institute of Technology, Brno, Czech Republic).

Ceramics used for the composite can be separated by its height. One series are consisted of 12 mm high ceramics (both casted and pressed). Other are 16 mm high hexagons. These ceramics hexagons were sintered at the temperature 1,550 °C and dwell time 120 minutes.

After the sintering process, surface was treated. This step was necessary since the wetting of alumina by aluminium is pour.

Seven hexagons were arranged into the honeycomb pattern. Position of the ceramic was fixed by a zinc coated iron wire.

### Aluminium preparation

A circle with diameter 125 mm was cut out from a two millimetres thin rolled sheet. Then five rectangles, 96 mm long and 72 mm wide, were prepared from a 5 mm thigh sheet.

In both cases sheets were made of a conventional aluminium with a high purity (AW-1050 H24, Al99.5, ALMS Brno, Czech Republic) Table 1 [18]. Although the use of such aluminium cannot be recommended regard to the low quality of the casted shape, surface and occurrence of internal defects, this material was used because of is its high plasticity and toughness. These properties are usually higher amongst pure metals rather than alloys. Another problem was caused by the high melting point of metal. That generates a high compression rate in the solid state which leads to an existence of a residual pressure.

Before casting, edges were neatened. It was done not only because of an esthetical aspect but the main reason was to reduce surface of the aluminium plate. Although only low concentration of $O_2$ is in the sintering furnace the oxidation process still exists due to high reactivity of aluminium.

### Gravity casting

The applied method of gravity casting is not a typical either. Unlike to the traditional way the batch of aluminium was not heated within form. Instead, ceramics and the form were placed into the furnace together with an input material. No filter was used as well as no gating system. These improvements should be probably added in the future.

The scheme in which ceramics and aluminium plates were inserted in a form can be seen in the picture 8.

The metal was melted by a retort furnace (XRETOR, U: 400 V, XERION Advanced Heating, Berlin, Germany). Inert gas of $N_2$ was applied during the process of casting, to reduce an oxidation reaction.

During the heating aluminium surrounded the ceramics and formed a jacket around it. Since there is no feeder-head the shrinkage always appears. But these defects have been partially pushed away from the body of the composite. This was achieved in previous studies by modifying of the thermal field during the cooling.

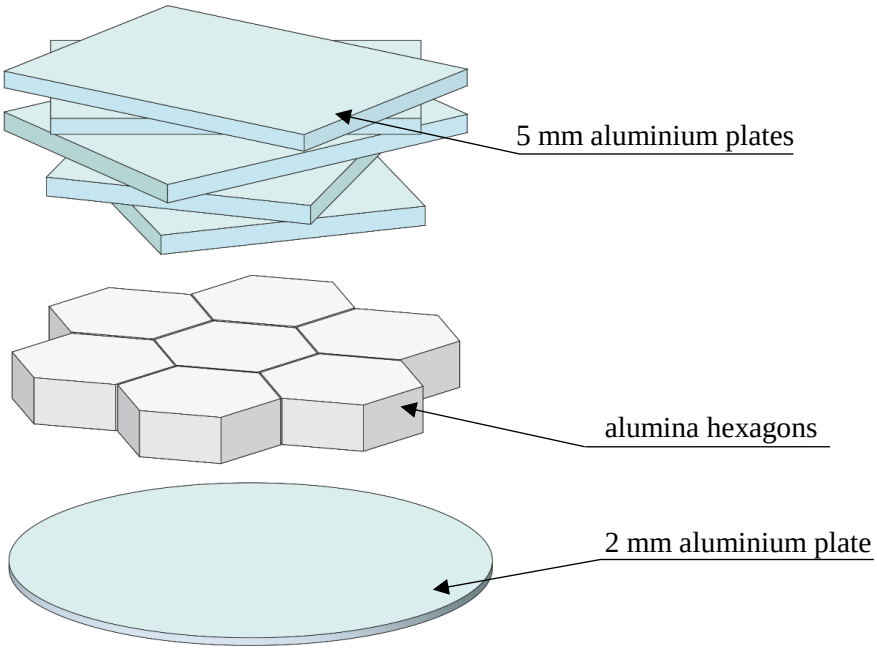


*Picture 8: A schematic illustration of the order in which the segments are placed in form*

The most visible factor which also effects the performance of the composite is the correct infill of the form. It is likely that the armour would perform better if spacing between ceramics are reinforced by the metal. Presence of aluminium in the spacing between alumina should help the transport of a shock waves and help to spread the energy in a larger area. Also, aluminium grid is expected to help keeping the fragments inside the armour.

Previously, dwell time on temperature of 900 °C was used during casting. However, this temperature seems to be too high when the melting point of aluminium is around 660 °C. To increase economy of the casting process, the temperature was decreased.

Problem with aluminium appeared in previous studies, when the metal did not enter the space between ceramics. To avoid this, surface treatment was applied. It was possible, that this problem will occur again, if the temperature of casting will by lower.

## 3.2 Ballistic testing

Number of composite specimens were prepared for 720 °C, 800 °C and 900 °C. There were two variants of ballistic shields. The on with contained 12 mm high alumina was tested according to the NIJ Standard-0108.01, armour type III. The second type with 16 mm ceramics was tested according to STANAG 2280, class A4 but the conditions were obtained by the combination of the threats contained in this level. The real conditions were: armour piercing projectile 12.7 x 108 mm, weight of projectile 48 g and velocity at 200 m was equal to 800 $m \cdot s^{-1}$. The kinetic threat was even more rough than the ones in class A4.

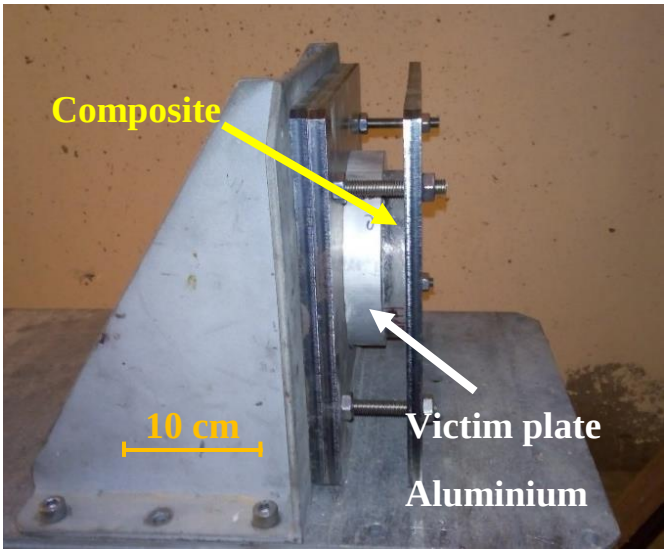


*Picture 9: Stand is holding the composite and victim plate, construction of the stand must by tough enough to withstand the impact*

*Picture 10: The velocity at 5$^{th}$ m was measured by a couple of triggers (prismatic construction), space between them was 1 m*

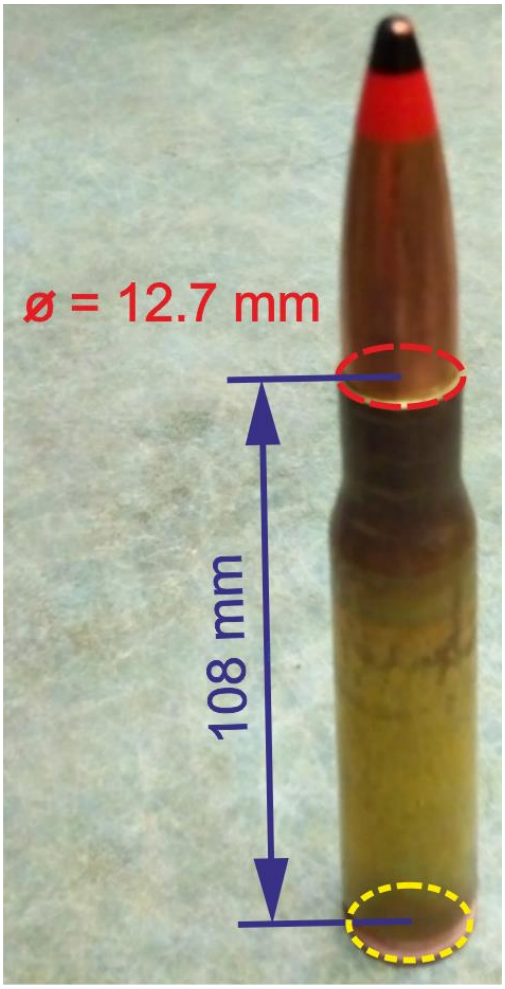


*Picture 11: Ammunition 12.7 mm x 108 mm which was used during testing*

### 3.2.1 Evaluation of fracture mechanism

Several samples were made from the locations where the crack has stopped its propagation. Obtained specimens were observed by scanning electron microscope. Examination was focused on phase boundary between alumina and aluminium which could be affected by a crack propagation.

### 3.2.2 Estimation of an areal density

The elemental hexagonal prismatic cell was defined for this task. The cell contains only one alumina hexagon. The height of the cell is the average value of the composite thickness. The spacing between ceramic is considered, so the base is limited by the middle of the joint. The layer of aluminium between alumina may differ. The thickness of aluminium between alumina moves from the 0.5 to 2.5 mm.

There were two versions of a composite. The first was made of 12 mm high alumina hexagons the other was made of 16 mm high ceramic. The base of the symmetrical hexagon was same in the both versions. 40 mm was measured between every two parallel edges of the base.

The volume of aluminium was estimated according to a geometry of the elemental cell and the ceramic which was inside. The mass of metal was counted according to a relative density of pure aluminium which is about 2.71 g·cm$^{-2}$. The average mass of alumina was measured out of the mass of seven hexagons.

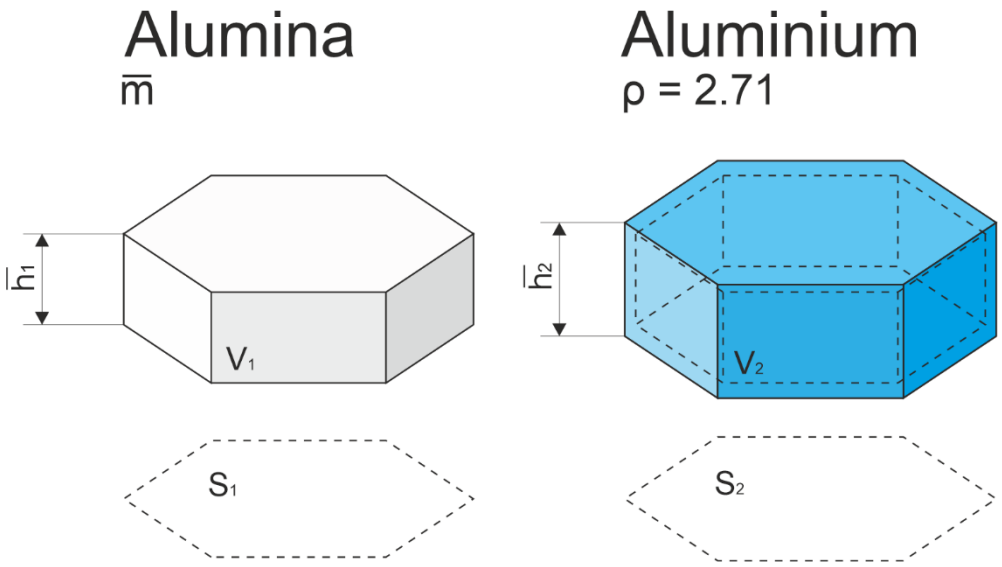


*Picture 12: A schematic illustration of the planimetric model used for the areal density equivalation*

**$Al_2O_3$ composite – 12 mm hexagon**

Areal density was estimated according to an average mass of the hexagon (61.7 g), thickness of the armour (1.47 cm), height of a hexagon (1.2 cm) and the density of aluminium (2.71 g·cm$^{-3}$). Depends on the spacing the value is about 5.10 ± 0.05 g·cm$^{-2}$ respectively 51.1 ± 0.5 kg·m$^{-2}$. This type of armour provides the protection again threat grade III (Dragunov rifle, 7.62x54R, v = 840 m .s-$^{1}$, m = 9 g) by NIJ Standard-0108.01.

**$Al_2O_3$ composite – 16 mm hexagon**

The average mass of the typical 16 mm tile is about 93.7 g, the thickness of armour 18.56 cm. As the thickness, nominal value was considered. The areal mass is theoretically 6.65 ± 0.07 g·cm$^{-2}$ or 66.5 ± 0.7 kg·m$^{-2}$ according to the geometry. This composite ensure protection against kinetic threats of 12.7 mm in class A4 in STANAG 2280. However, its properties are high enough to provide protection against combination of a maximal velocity and a mass for this calibre (12.7x108 API B32, $v_{200}$ = 800 m·s$^{-1}$, m = 48 g).

## 3.3 Four-point beam bending adhesion test – specimen preparation

### Preparation of the alumina suspension

During this task aluminium tiles from suspension containing 55 vol. % of alumina was prepared. The suspension is consisted of five compounds in total: PVA (polyvinyl alcohol), Darvan, octanol, sucrose and $Al_2O_3$ powder. High purity (99.8 %) powder SUMITO AES – 11C α $Al_2O_3$ (Sumitomo chemical, Tokyo, Japan) was used in the process. The particle size declared by company was 0.3 μm.

In the current order compounds were added and mixed into the bottle in defined amount. The recipe was designed in the previous research [38]. All compounds can be seen in the table 5.

| | |
|---|---|
| 1 % PVA | 51.55 g |
| Darvan | 4 g |
| Octanol | 3 drops |
| Sucrose | 10.10 g |
| $Al_2O_3$ powder | 270,0 g |

*Table 5: Suspensions compounds list [38]*

Sucrose was added in the form of powder and dissolved.

Alumina or zirconia balls with diameter approximately 4 mm were implemented to boost mixing effect in the next phase. Then the alumina powder was poured into the bottle and properly mixed. The final suspension was mixed on the ball mill for three days.

### Preparation of molds and slip casting

Plaster for mold was made by mixing a water and plaster of Paris in a ratio of 3:2. Typical batch was consisted of 200 ml of water, 15,6 g of cement and 300 g of a gypsum powder. First required volume of water was poured into the bowl and mixed with cement. The plaster was added when the cement was dispersed properly.

Then fluid was casted immediately. Current composition of fluid had caused that the plaster started to harden very quickly and any dwell time would cause the radical increase in viscosity. After five minutes the plaster loses its ability to be poured and after another fifteen minutes it became hard enough to be removed. Fluid was poured into the frame made of popular Czech plastic construction toys Cheva. The frame was fixed on a vibrating table by a hot melt glue gun. Vibrations during the pouring unsecured that the plaster of Paris entered even corners and other difficultly accessible locations. Besides it helped to escape to bobbles of $CO_2$ (the product of reaction) and absorbed air.

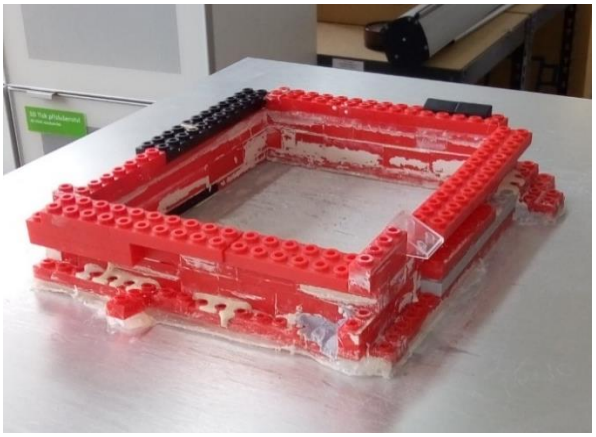

*Picture 13: The frame from the Cheva prepared for pouring of plaster of Paris*

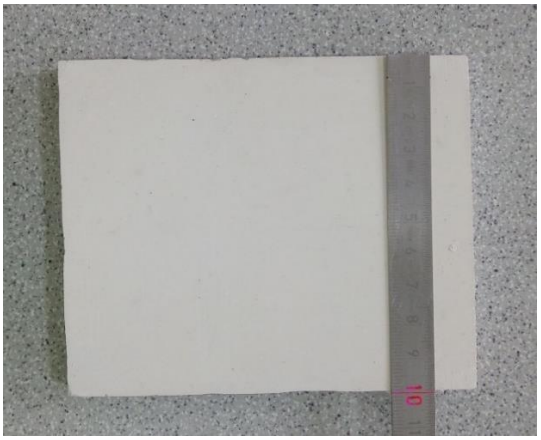

*Picture 14: One segment of recently dried, the number on the scale represents ten millimetres*

After 20 minutes plaster molds were removed and placed in the drier. At least three hours molds were subjected to condition inside the drier which were set to 40 °C.

Dried tiles of plaster were honed by a 200# sandpaper carefully, till the surface became smooth.

The rest of mold was made from another two parts which were shaped by 3D print. Because of the compression during a dehydration of the slip cast, feeder head is needed. Size of the slip cast was limited by frame which was also made of plastic.

Every surface of plastic must be lubricated before it gets in touch with alumina suspension. On this record Teflon spray was used.

Finally, all parts of mold were assembled. Plastic frame was stick on the feeder head with chloroform. The bound is relatively weak, so the parts can be separated quite easily. Then the frame was enclosed by the plaster plates. For need of disassembly the plaster plates and frame were fixed together by the Ratchet Bar Clamp.

The lifespan of the mold is limited by the number of uses. During the slip casting the pores are getting clogged up, losing their ability to absorb water. After every use plaster plate must be dried and honed again. If the plaster tiles were not used more than five times, they can be used again. Using the same tiles after more than five reciliations cannot be recommended, since the drying properties are unpredictable.

After 72 hours of rolling, the suspension is almost prepared to be casted. The only step missing is the vacuuming of the slurry. It acts just at moment before casting to ensure the lowest possible level of dissolved air. The suspension boiled due to the low pressure. Vacuuming last only few minutes. Longer dwell time would lead to decrease of the $H_2O$, causing the suspension starts hardening untimely.

When the suspension was ready it was casted into the plaster mold. During casting the vibration table was used. It helped the suspension to infill the mold properly. The feeder-head was covered by microscope slides. That stops the $H_2O$ vapor to escape the feeder-head, guarantee that the suspension rest of the mold can be still supplied by a “fresh” slurry.

Depending on the ceramic tile thickness, suspension properties, mould health and climatic condition the hardening usually took 5 – 6 hours. After that time the mould was opened. The feeder-head was cut after the opening. The green tile was brushed and transported into the climatic room where it was subjected for 50 hours to more stabilized conditions.

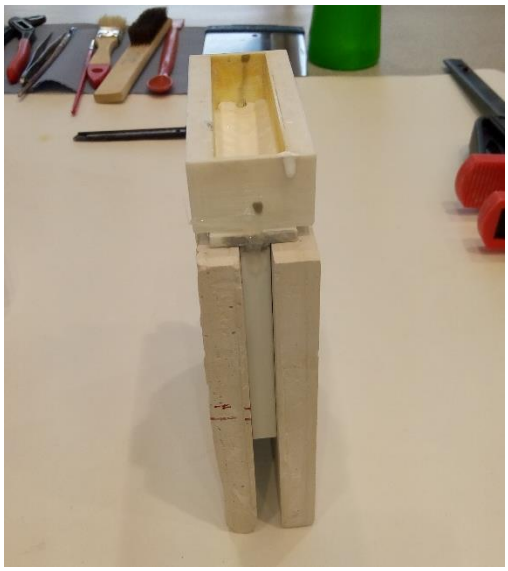

*Picture 16: Mold prepared for opening*

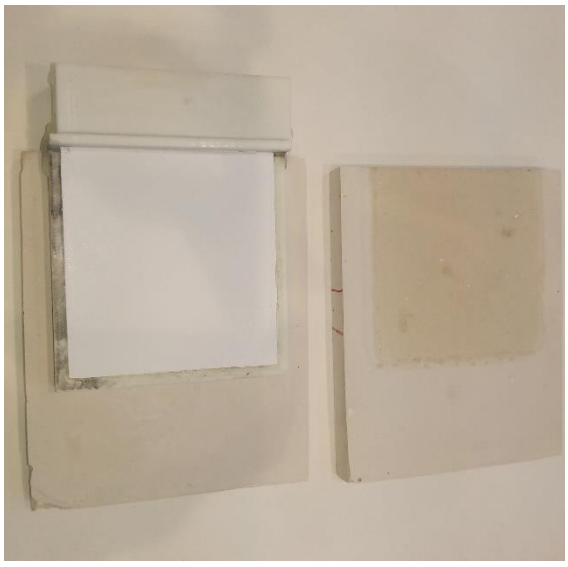

*Picture 17: Disassembled mold, greenbody*

## Pre-sintering and sintering

Green body was placed in to the “low” temperature furniture and heated on to the 700 °C for 60 minutes. By this process the binder is degraded and removed.


*Picture 18: High temperature furnace (Classic – 18000C, Czech Republic)*

The last step before sintering was the finishing process. The tile was cut into estimated dimension, so the size after sintering was 8 x 35 x 50 mm. The solidification was caused by the sintering was approximately 16 %. That means that the dimension of the tiles, before sintering must be 9.3 x 41.6 x 59.5.

Ceramic was sintered by high temperature furnace (Clasic - HT18000C, Czech Republic). Heating program is shown in the graph below.

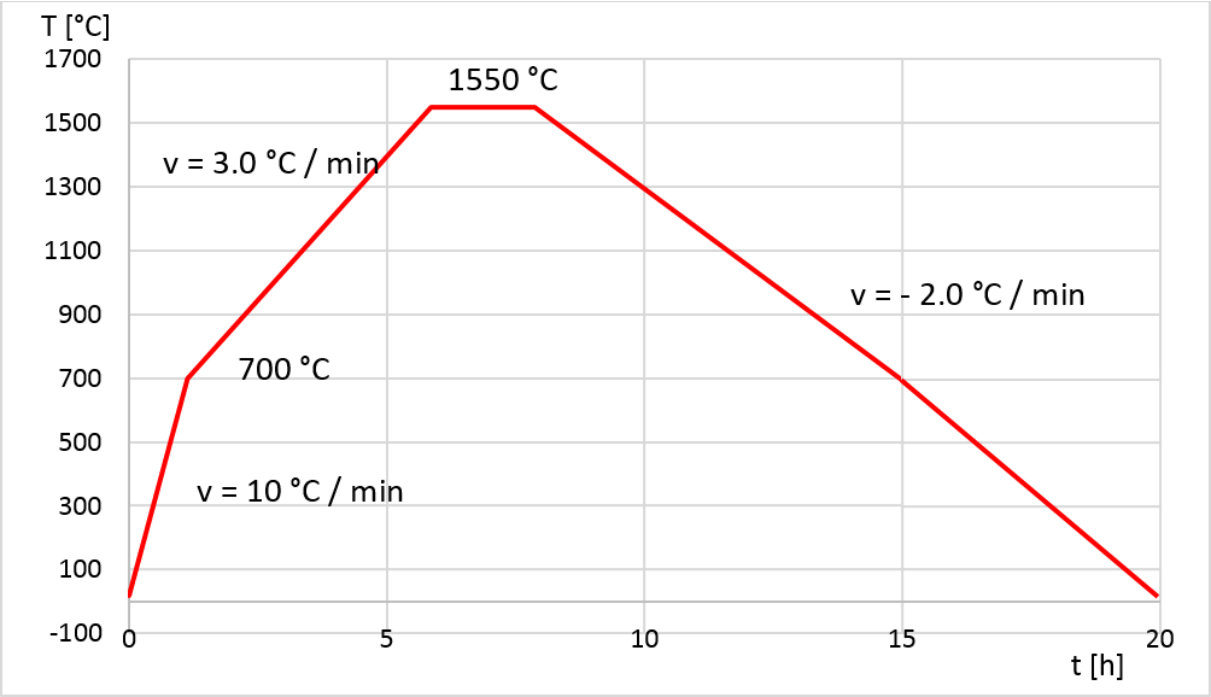


*Graph 1: Heating program during the sintering*

### Gravity casting

For the task of the experiment more simplified version of gravity casting was used. Unlike to the traditional way the form was heated in the furniture together with the batch of metal. The form was a graphite cylindrical crucible with diameter of 130 mm and 40 mm deep. The form did not contain the feeding head. The shrinkage was expected to occur in the higher level of the form, so it would be machined.

The existence of the wrong solidification often caused problems in the previous research focused on the composite armour. Spaces without aluminium occurred in the node areas between ceramics, reducing the effectiveness of the armour. So, there was an effort to modify the thermal field during cooling of the metal. One-centimetre graphite felt insulation was used for that task in the first attempts. The felt was located on the very top of the form. The plan was to decrease the thermal transmission from the upper parts of melt. The solidification process would start at the bottom of the crucible ideally. Then the shrinkage would appear in the upper level of the material.

### 3.3.1 Optimization of the preparation technique

In the following part specimens will be not named chronologically according to date in which they were prepared. Instead specimens will be marked in a retrospective manner. The alphabet naming was chosen just for a better orientation in the text. Also, the system of marking should represent quality of the specimens.

The casting schema was similar to the one which was used of composite. The ceramics were fixed together by zinc coated iron wire and placed between aluminium plates. The importance of notch, pre-crack and strict geometry generated specific problems and solutions.

**Specimen F**

In the first test two alumina tiles were bound together by a zinc-coated wire. The spacing between ceramics was filled by a graphite paper to prevent it will be untouched by metal. For the same reason, the future pre-crack (10 mm wide) was drawn by graphite.

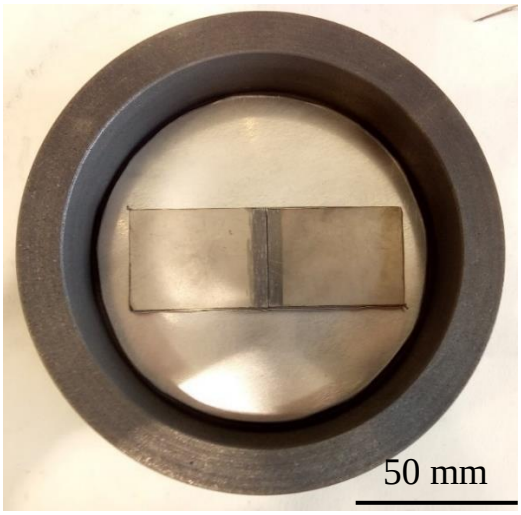


*Picture 19: Setup before casting, before adding aluminium plates*

The order in which the samples were placed into furniture is showed in a picture 19.

After the casting process when the specimen cooled down and a redundant material was removed from the sample by a bandsaw.

The first attempt (specimen F) ended unsuccessfully. The main problem was caused by a contraction of aluminium. That effect caused a deformation of the sample which was bended in a 175-degree angle. Besides, cracks occurred in the alumina. These cracks were probably caused by a residual stress induced by a compression of the aluminium. Also, the preparation of the notch and the crack appeared to be insufficient.

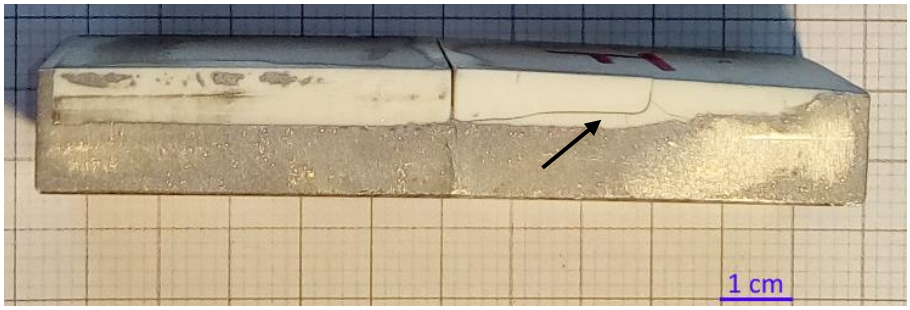


*Picture 20: Specimen F, after milling, the black arrow shows the crack in ceramic*

**Specimen E**

Nonstandard ceramics was used in the next experiment. Their width was about 28.3 mm instead of 35 mm. Also, four 1 cm wide graphite papers of at total thickness of 1 mm were placed underneath the both alumina tiles. It made a middle of the ceramic raised and reduced the angle caused by a compression of the metal followed by deformation. Also, the crack zone was covered by 1.5-millimetre wide stripe which was anchored on the both sides.

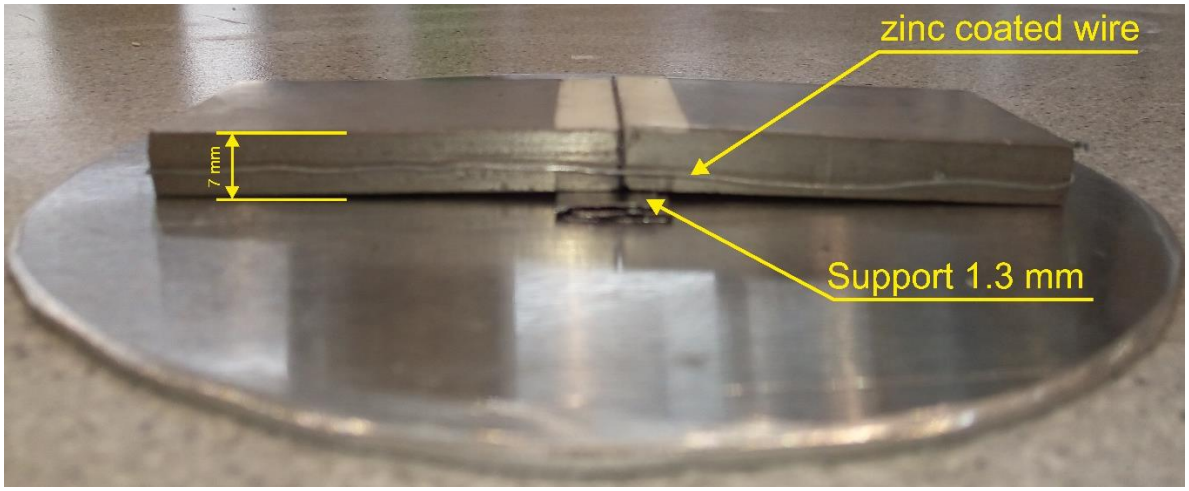


*Picture 21: Specimen F, the centre of ceramics was supported by graphite paper to compensate the deflection due to the compression of aluminium*

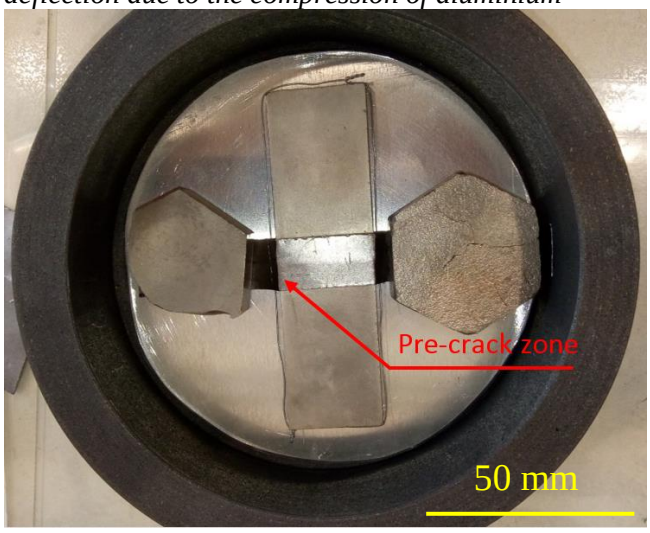


*Picture 22: Specimen F, the pre-crack was prepared by the graphite paper, paper is anchored by weights*

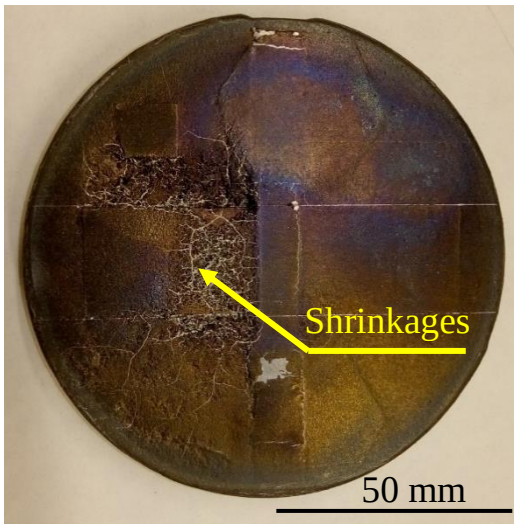


*Picture 23: Specimen F, the cast, zone affected by shrinkages occurred*

Accidently the shrinkage appeared in the middle of cast, so a significant part of final specimen was afflicted by cavities.

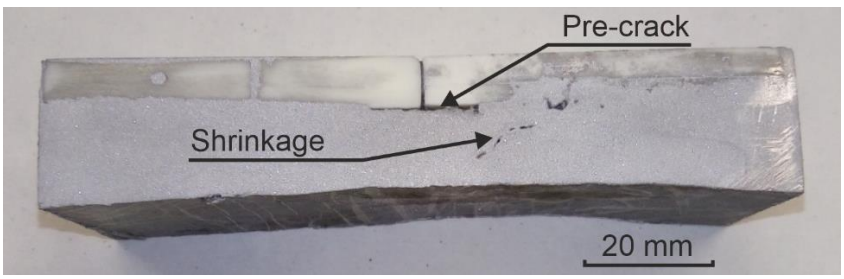


*Picture 24: Specimen E, body of the specimen was affected by shrinkages, the pre-crack was achieved*

**Specimen D**

During the third attempt larger volume of graphite felt was used. Additive insolation was placed on the top and around the form. This volume of insulation represents the insulation grade A (see Appendix II.).

Improvement of the shrinkage location was expected, by this modification. However, it did not happen.

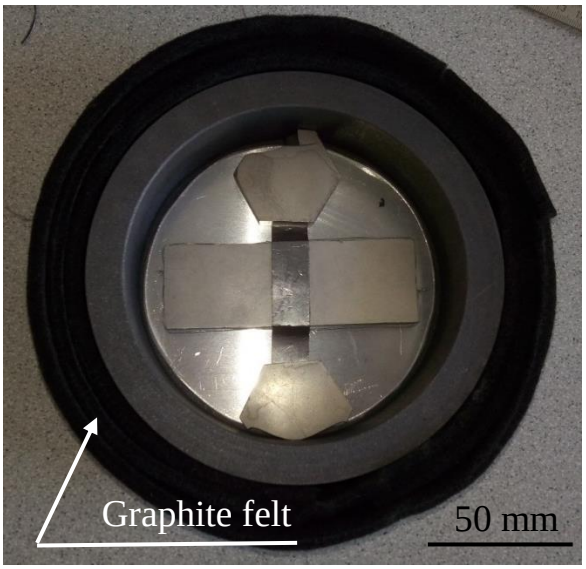


*Picture 25: Specimen D, composition in which segments were put in furnace*

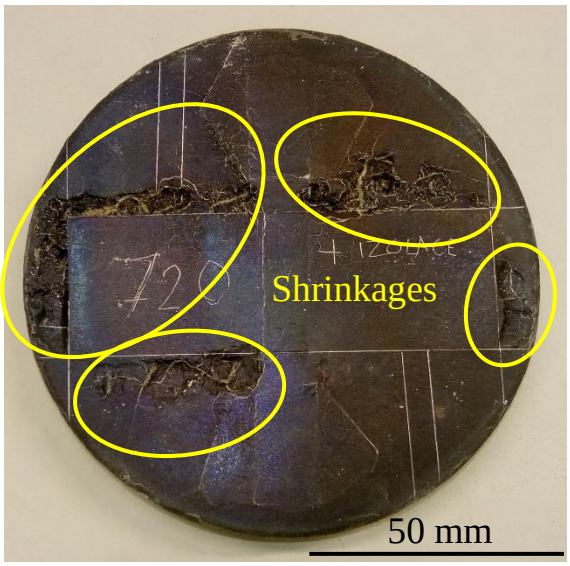


*Picture 26: Specimen D, the cast, zones affected by shrinkages still occurred*

Although the insulation was increased shrinkage appeared in the central sector again Picture 26.

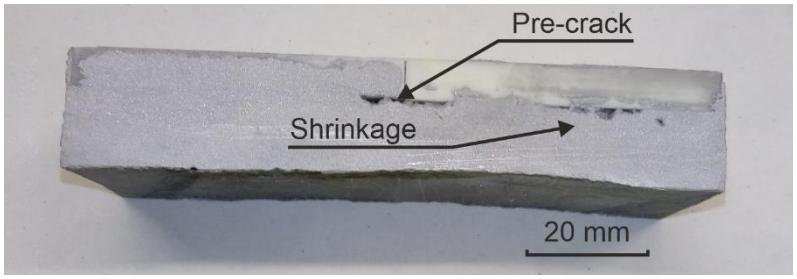


*Picture 27: Specimen D, body of the specimen was affected by shrinkages*

### Specimen C

Different temperature was used at the fourth attempt. Specimen was casted at 800 °C. B type of insulation was used (see Appendix II.). There was no visible shrinkage in the body of the specimen seen after cutting.

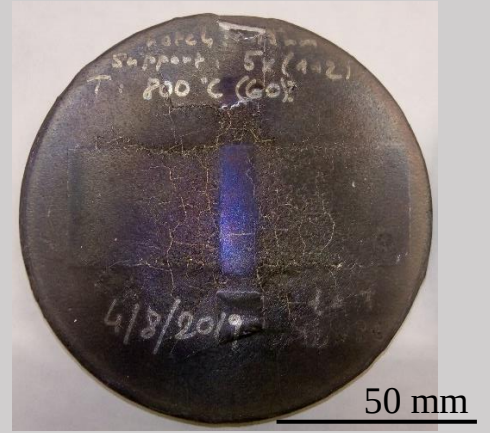


*Picture 28: Specimen D, the cast no problem with shrinkages*

### Specimen A, B

Both specimens were made at the same conditions. The highest insulation grade was used to ensure that the process of solidify will be slower at the upper part of form. The longer dwell time on the 720 °C were applied. The time prolongation should help aluminium to enter all cavities. Besides, prolonged dwell time at temperature had a positive effect on the deformation caused by the compression of aluminium. It is likely, that it has also positive effects on a residual stress.

Specimens did not suffer by shrinkages as far as it can be told from the visual observation.

When the all six specimens were made, they undergone another shaping process. Before testing aluminium faces were milled. So, the specimens received their final shape. Despite the effort with was made to reduce the angle in which the specimens were bended, the axis was never straight precisely. The thickness of the specimens altered for that reason. The thickness was always 16 mm at the middle, however the thickness at the end of specimens is various.

The thickness at the middle of specimen was weakened in the case of F and C. The reason was a convex shape of the surface on the top of the cast. In both cases thickness was lowered by one millimetre approximately (See appendix IV.).

Side face of samples was grinded before test to ensure a better visibility of crack propagation.

## 3.4 Testing conditions

The Four-point beam bending test was done by using a universal low strain rate testing machine INSTRON 8862 (Illinois Tool Works Inc., University Ave, Norwood, United States of America). The loading span was ½ of a support span. The support span was about 80 mm. The room temperature during testing was around 22 °C. The speed in which the beams were deformed in the vertical direction was set to 0.5 mm·min$^{-1}$. The testing of specimen was stopped, when the value of the flexure stress decreased radically and there was no hopeful indication for reversal or when the value of extension reached 7 mm. This was a limiting value, since the change of geometry would lead to a different mode of loading. The specimen would be loaded in shearing instead of flexural.

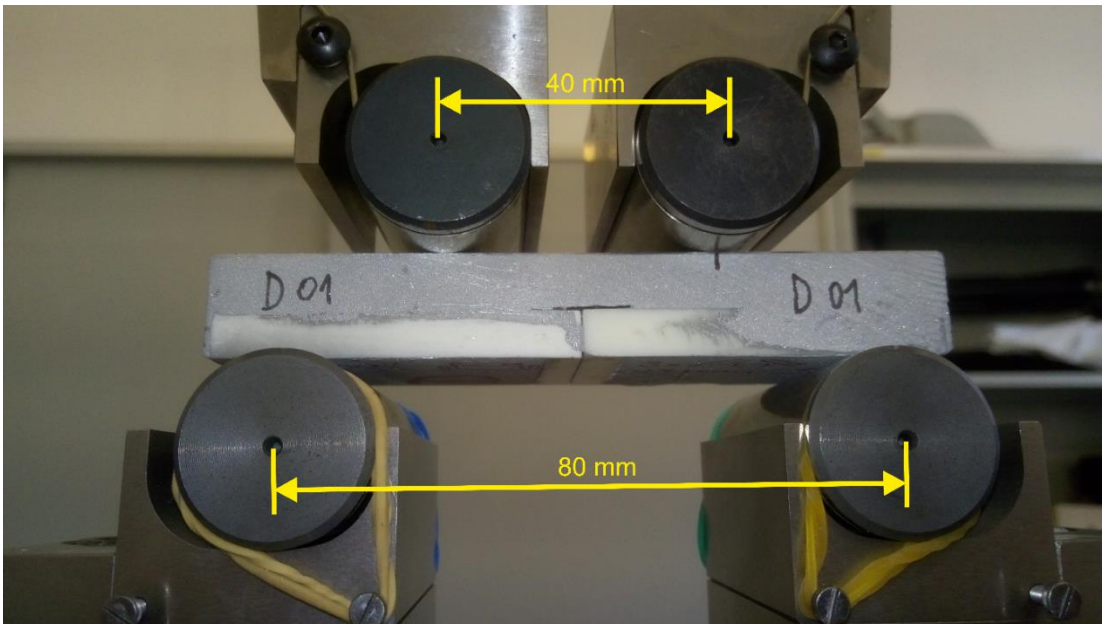


*Picture 29: The setup of the modified 4PBT test, support span 80 mm, loading span 40 mm*

## 3.5 Preparation of the metallographic samples

Beside the mechanical testing microstructure analysis was made. The plan was to describe the grain size and to observe the structure after solidification.

Samples were usually extracted from waste material from casts for 4PBT. For the task of comparison samples were cut out from the similar location in the cast. Six of them had fully metallic character. The other was cut through the interface of alumina and aluminium. The only one sample was received from the body of ballistic specimen which was subjected to a kinetic energy of projectile.

See Appendix III.to receive more information about sample selection.

Samples were mounted by polystyrene, the maximum temperature during process reach 215 °C. Eight samples were prepared in total.

Samples were grinded and polished by a Struers machine (Struers Pedemin, Struers, Tokyo, Japan) according to an Appendix III.

Deep etching was applied to reveal the primary dendritic microstructure. The aqueous solution contained these acids in current proportion:

HCl – 45 ml

$HNO_3$ – 15 ml

HF – 25 ml

# 4 RESULTS AND DISCUSSION

## 4.1 Composite preparation – temperature program

The aim of these experiments with temperature programs was to achieve an optimal temperature during the casting. Because of the higher density of alumina ceramics, hexagons were placed at the bottom of the form. The space between ceramic should be infilled by aluminium ideally. Furthermore, position of the shrinkages should be outside the body of the composite. Both parameters should be fulfil at as low temperature as possible in regard to increase the energetical efficiency of the process without a negative effect on composite properties.

Composites were prepared at temperatures 900°C, 800°C, 720°C, and 680°C with dwell time 30 minutes. The results are shown in picture 30, picture 31, picture 32, and picture 33, respectively.

The highest experimental temperature 900 °C did not provide a complete infill of spaces between alumina and empty places are visible in the material of composite, see picture 30. Shrinkages occurred at a suitable position at the edge of the sample.

In the next experiment, temperature was decreased to 800 °C. No problems with casting fluidity occurred and space between ceramics was infilled properly as it can be seen in picture 31. Also, shrinkages appeared in the suitable zone near the edge of specimen.

In the following experiment (see picture 33) temperature was decreased by another 80 °C. No problem with casting fluidity appeared again. Even the occurrence of shrinkages does not cause any problem because they were located at a suitable location.

Hence no radical difference between composite casted by 800 °C and 720 °C was found, the casting temperature was lowered again at the temperature of 680 °C. The result proved the setup as inappropriate. As it is showed in picture 33 the viscosity of aluminium was high, so the aluminium did not coated ceramics properly.

The lowest applicable temperature seems to be 720 °C. Although the quality of cast is not only affected by the maximal temperature, but other factors can modify the result significantly. The dwell time, thermal transfer between crucible and furnace and surface treatment played an important role in the casting process.

Temperature 680 °C appeared to be too low, despite to the fact that the melting point of the current aluminium was excited Table 1 [18]. This has probably several reasons:

- Although the metal was melted its viscosity was too high, so the dwell time scale was insufficiently short to ensure a required quality of cast.
- There is a probability of contamination of melt during the cast process. However additive compounds usually decrease the melting temperature of the alloy the different effect might happened.
- The process of casting was not an ideal. The metal was not casted really, but it was presented in the form all the time. The method is more similar to sintering process indeed. However, the nitrogen atmosphere was used the aluminium surface was covered by the oxygen layer which decreased the fluidity of molten metal.
- The real temperature inside the crucible is unknown because the location of sensors. Besides, the thermal field was affected by a nitrogen flow.

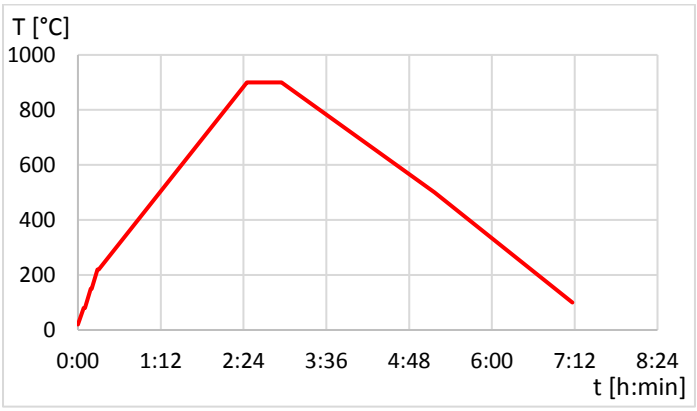


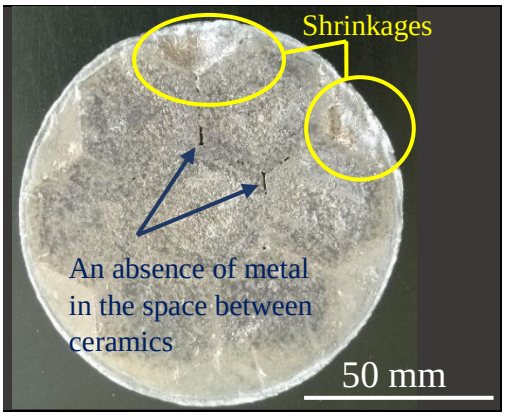


*Graph 2, Picture 30: Heating program 900 °C, 30 min dwell time*

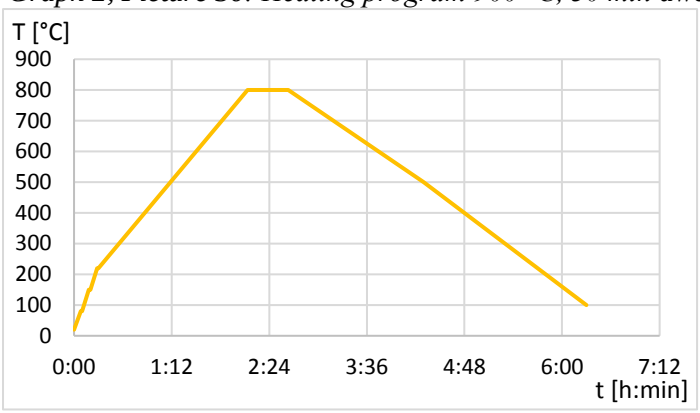


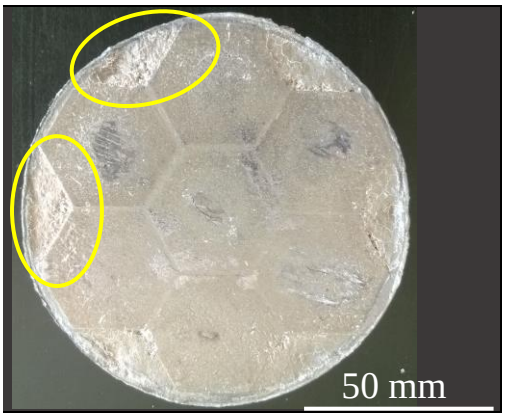


*Graph 3, Picture 31: Heating program 800 °C, 30 min dwell time*


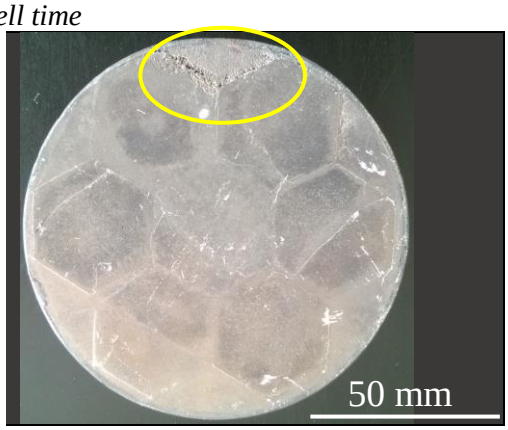


*Graph 4, Picture 32: Heating program 720 °C, 30 min dwell time*

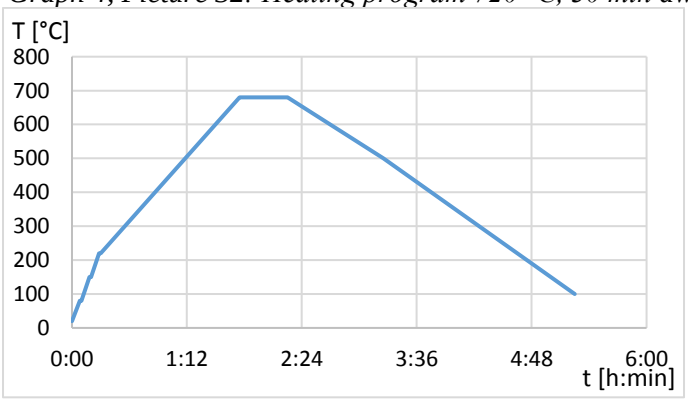


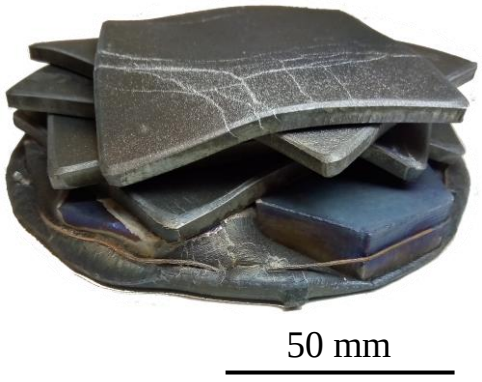


*Graph 5, Picture 33: Heating program 680 °C, 30 min dwell time*

## 4.2 Ballistic testing – fracture analysis

This test was focused on the behaviour of the interface after dynamic loading. The motivation of the experiment was to the information about toughness of the interface. Scanning electron microscope SEM was used in analysis for its high focal depth.

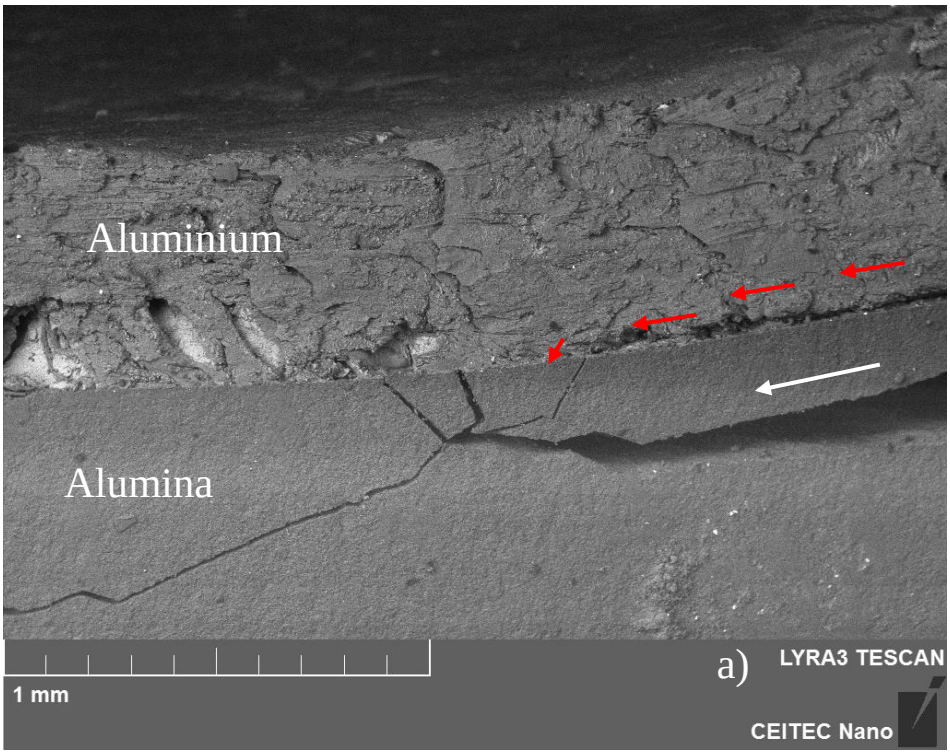


*Picture 34: BSE image, ceramic – metal interface, low fracture toughness caused that the crack propagated mainly through the ceramic, white arrow shows a direction in which the crack propagates, red ones shows a direction of the parallel crack which followed the interface for a while*

Secondary and Backscattered electrons were used for the observation of fracture mechanism in vicinity of interface. Low fracture toughness of alumina caused that the crack propagated mainly through the ceramic a). The performance of the interface was good according to these pictures. The corruption of the interface was noticed only in picture a). Fracture of interface appeared in the zone where the damage to ceramic was high. Then the crack changed a direction and ran in to the ceramic.

In the picture a) and b) are visible holes. Theirs origin are probably micro-shrinkages. The backscattered electron image showed a contrast between pores and aluminium matrix. That indicates a presence of an atoms with a higher atomic number on the surface of cavities. The chemical difference might by caused by a segregation of the components dissolved in melt.

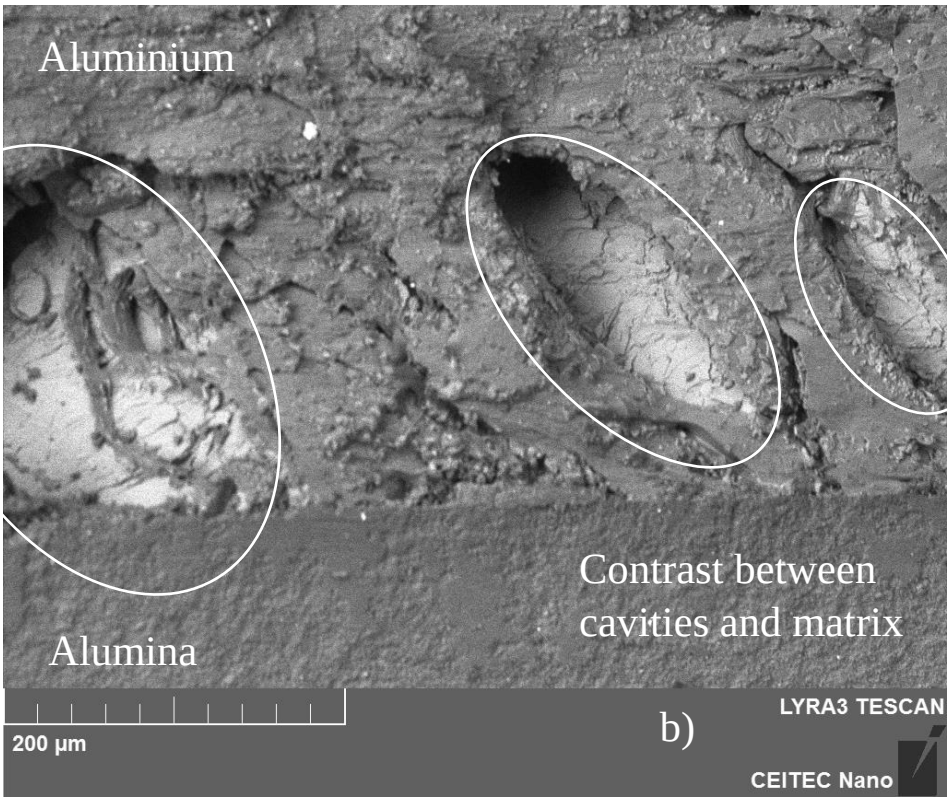


*Picture 35: BSE image, ceramic – metal interface withstanded the dynamic load, light areas shows presence of different compounds on surface of pores*

Compare with literature [40], Picture 36 we can see the propagation of the crack directly by the 7B52 / 7A01 interface. This laminate was processed by a hot rolling and by a peak aging and was shot by 7.62 mm WO-109C armour-piercing incendiary according to GJB 59.18–88. A different behaviour of composite was caused by a different ballistic condition, rigidity of an armour and by a strength of joint.

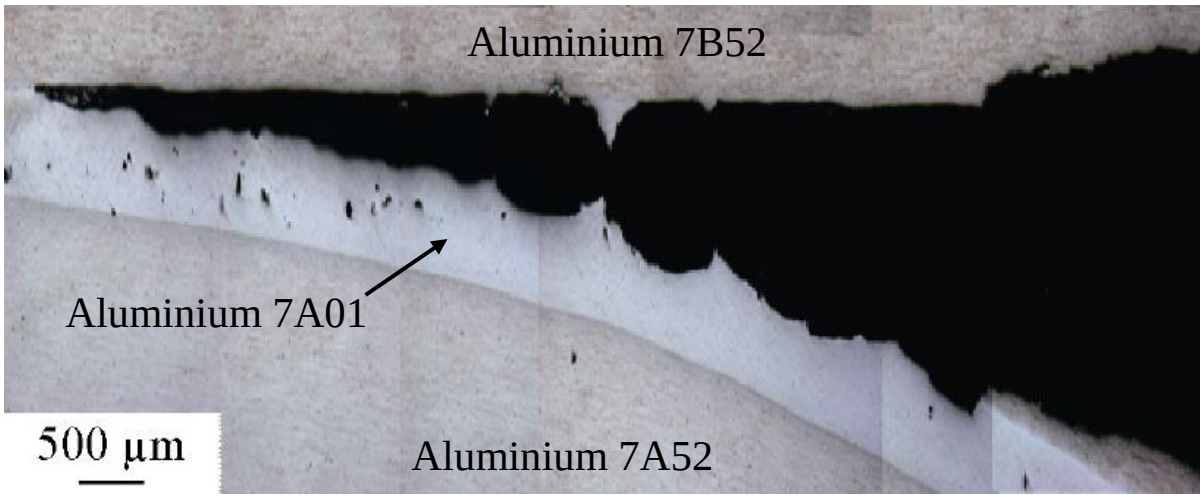


*Picture 36: OM images of tearing fracture in 7B52 layer [40]*

## 4.3 Modified four-point beam bending test

Specially designed four-point beam bending test was applied to quantify adhesion between alumina and aluminium. The need for this information arose because the adhesion energy is an important factor effecting the performance of the composite.

The need for sufficient dwell time and the temperature transfer was proved by the experiments because the absence of running system generates a risk of shrinkages. Even the low level of thermal insulation and 30 min dwell time on temperature 720 °C helped in the case of ballistic composite. However, this was not enough in case of 4PBT specimens.

It is important to know the crack position during the loading for evaluation of the energy. However, crack propagation along the interface was undetectable even when the side face of each specimen was grinded. This problem, probably caused by insufficient quality of a diving line, led to the fact that it was not possible to measure the adhesion energy. So only data about flexure strength over extension were obtained.

Serie of six specimens was tested in the conditions which are written above. From the measured values a diagram of dependence of flexural stress to an extension was made for each sample. Although, these graphs do not describe the consumption of energy during the propagation of crack, they can be compared. The early stage of diagram is nearly identical or similar for all specimens which were made by the same thermal process. The difference between these diagrams appears when the flexure stress excites the critical value needed for the crack propagation. Then the smooth character of the curve is disrupted. The steady increase of the flexure stress indicates that the material is hardening due to plastic deformation. This process is continuing even when the crack is growing. However, the crack length affects negatively the resistance of the material. That leads to a deviation inside the diagram or it changes a direction of the curve.

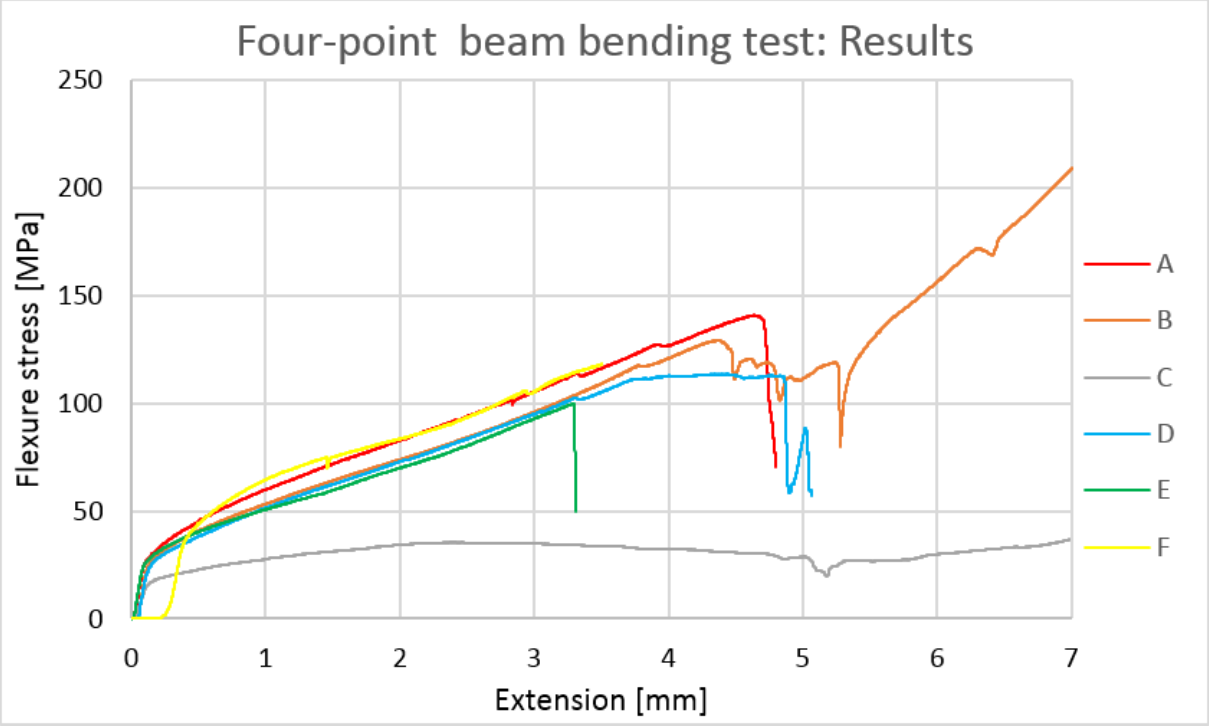


*Graph 6: Diagrams shows behaviour of specimens during the loading, all specimens prepared by 720 °C (A, B, D, E, F) have a similar development of flexure stress over extension at the early stage of test, performance of 800 °C (C) is low*

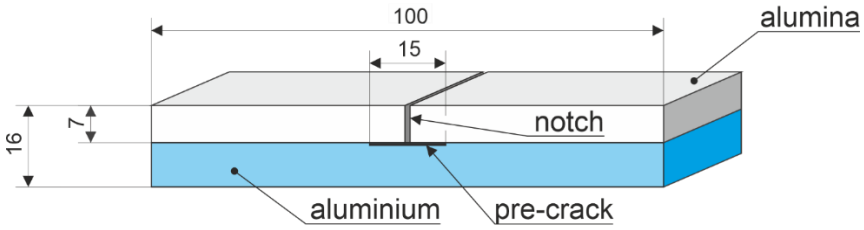


*Picture 38: A schematic illustration of the specimen for the modified 4PBT, the existence of notch and pre-crack prevent the flexure strength to being measured by the experiment instead of delamination energy*

| Specimen | A | B | C | D | E | F |
|---|---|---|---|---|---|---|
| Temperature [°C] | 720 | 720 | 800 | 720 | 720 | 720 |
| Dwell time [min] | 60 | 60 | 30 | 30 | 30 | 30 |
| Pre-crack length [mm] | 15 | 15 | 15 | 15 | 15 | 10 |
| Width [mm] | 36.23 | 36.98 | 37.5 | 36.17 | 28.34 | 37.4 |
| Thickness [mm] | 15.50 | 15.92 | 16.17 | 15.79 | 16.24 | 16.30 |
| Insulation type | A+ | A+ | B | A | C | B |

*Table 6: Selective description of specimens' properties*

| Specimen | Comments |
|---|---|
| A | Local defect on the aluminium face - pinhead approximately |
| B | |
| C | Imperfection on the aluminium face - 2 $cm^2$ approximately |
| D | Existence of shrinkage |
| E | Atypical width of specimen, existence of shrinkage |
| F | Existence of cracks in the ceramic, imperfection on the aluminium face - approximately 2 $cm^2$, pre-crack prepared differently |

*Table 7: Other information about specimens' which were not mentioned in the Table 6*

The yellow line represents the behaviour of the specimen F during the test. The early end of the test was caused by the corruption of the ceramic. The collapse was caused by the cracks which existed in the material even before the start of the test. There is a difference between the F line and lines A, B, D, E at the first 0.5 mm. That is probably caused by a different method of pre-crack preparation. Unlike the other specimens the pre-crack was not fully developed by the graphite paper. Instead the only the bound between ceramic and metal was weakened. However, it was not expected much from the specimen F. Its character cannot be considered as representative since quality of the material was low. Its asymmetrical thickness caused a three-point bend at the very beginning of the test. However, this specimen suited well as a pilot sample for a test condition setup.

A grey line represents a specimen prepared at 800 °C. Cracks appeared at the location of the pre-crack during the testing. The direction in which the cracks were propagating did not follow the interface of the both materials. It ran into the metal under an angle of 90 ° against the axis of specimen.

*Picture 39, 40: Rupture of the specimen C was caused by the propagation of a crack through the*

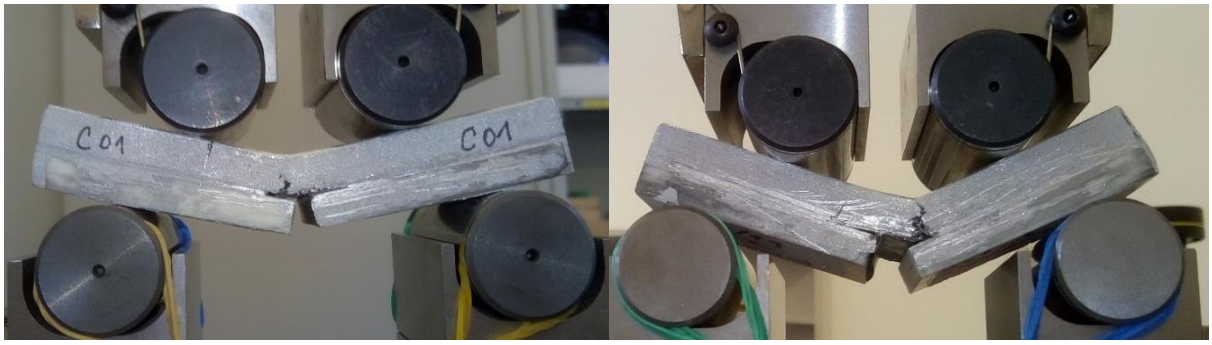


*aluminium*

The resistance of the specimen was the lowest. It is an only sample which was made by this temperature so it cannot be said for sure that the problem is in the thermal process. There is a possibility that the other influences took place because the casting process and specimens' geometry is not ideal. Also, the impurities on the surface of the aluminium must be considered. The flexure stress was counted according to the theoretical thickness of an aluminium however the real thickness was slightly different (see Appendix IV.).

A, B, D, E performance is quite similar on the beginning of loading. They were all casted at the temperature of 720 °C, but they differ by the time of dwell time and by insulation used during casting. The material was visibly affected by the defects.

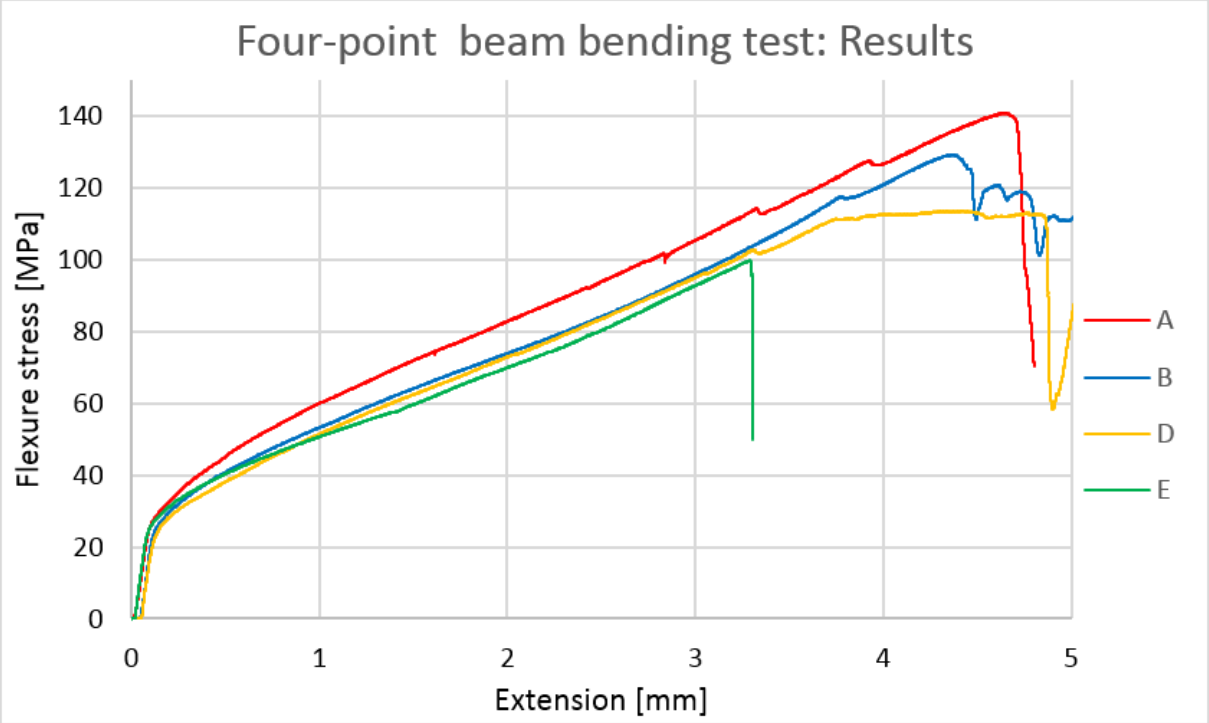


*Graph 7: A detail on 720 °C specimens, specimen F is not included for its low quality, so the poorest performance provided specimen E which was prepared without insulation, the highest resistance against flexure deformation and crack propagation was noticed in case of specimens A and B, they were both prepared with an extra insulation and longer dwell time on temperature*

*Picture 41, 42: Highlighted area enclose the cracks which occurred on specimens, D and B*

The resistance of the specimen E was the lowest from these four specimens and second lowest at all. When the flexure stress reached the 100 MPa it immediately started to decrease.

Also, in the case of curves A and D deviation had been generated by the similar stress. Although the smaller departures from the smooth character of curves were visible even before. Only the curve B did not change much under that condition but changed 18 MPa later.

The radical change in the resistance of specimens A and B appeared between 4.3 and 4.6 mm. These changes are most probably connected with cracks propagation. Performance of specimen B stabilized after some time and start to increase again.

There is likely that the cracks did not following the interface, but they ran in to the metal. On the side face of the specimen A and B crack occurred perpendicularly to a specimen axis. These crack however may just exist on the surface because of the hard oxidic layer on the aluminium surface. Different cracks appeared on the surface of specimen D.

The deviation of the crack from the interface cannot be proved just by the visual observation. Because of that specimens will be subjected to non-destructive analysis. One of the testing methods suitable for the need of finding of crack tip is ultrasonic testing.

The application of modified 4PBT was encouraged by researches M. Zhe, O. Dezellus, G. Parry, M. Braccini & J. C. Viala (I. in the following text) [41] and N. Suansuwana, M.V. Swain (II. in the following text) [37]. Test method provided a satisfying result in these studies. One of the reasons why the effort made for measuring adhesion energy did not bring a successful result is the form of pre-crack. On regard to the fabrication process of composite it was difficult to prepare proper tip of the crack. The edge of the pre-crack should be perfectly sharp and focused in the interface ideally. Instead the crack tip was made in measurable radius. In the case of research I. [41] pre-crack was prepared by a chemical treatment of the surface followed by initialization of the crack by three-point bending test. A kind of surface treatment was applied on the first specimen F. However, the curve character did not change much. In another case II. [37] pre-crack was induced by limited number of loads and partial unload cycles [37. 41].

Nevertheless, these techniques are useful if the properties of the adhesive bound are weaker than the both materials. In the study I. [41] adhesive layer was known as the brittle one. The task of the study II. [37] to improve the bound between titanium or titanium alloy and the porcelain because it is so weak. The basic requirement for adhesive toughness was fulfilled in these experiments.

If it is other way around the crack starts to move in the most convenient direction, which leads though the weakest material. That is probably case of the experiment in this thesis. The measurement of adhesion energy failed because interface had a better property then it was expected and because of the lower quality of aluminium which is prepared by a nonstandard process.

## 4.4 Microstructural analysis of aluminium matrix

The motivation of these analyses was to verify the quality of the aluminium. As it was written above the technology of casting was not ideal. The task was to collect a preliminary information about the structure of the material and to find possible dangers of the current setup. These information will be used in a subsequent research.

### 4.4.1 Optical microscopy

First, samples were observed in the non-etched state.

720 °C, 30 min
Insulation A

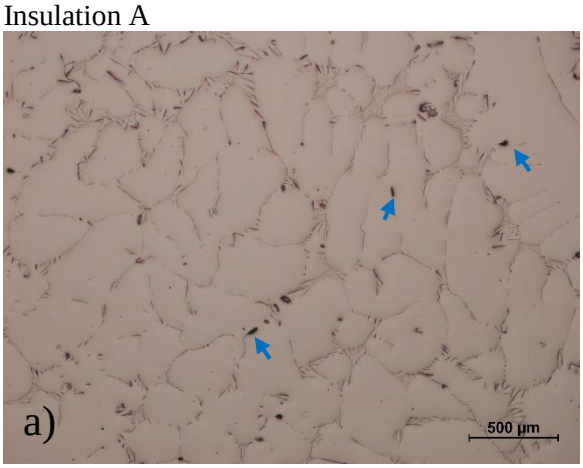


Insulation C

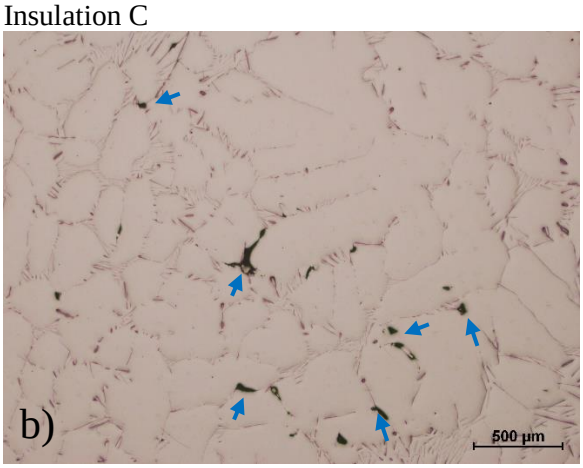


*Interface, non-shot, insulation B*

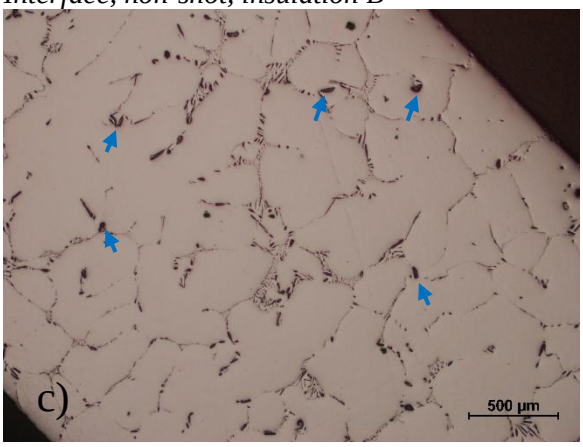


800 °C, 30 min, insulation B

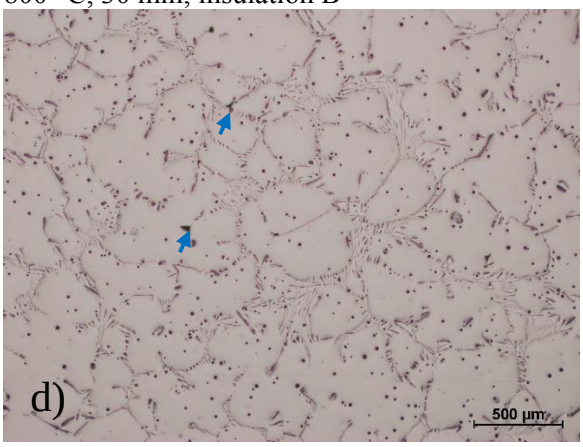


*Picture 43 - 46: (a) – d)) a dendrites structure which are highlighted by a intermetallics appeared in the all samples, the larger amount of intermetallics was found in the picture c), the size of dendrites is a similar across a) – d), in all pictures pores (blue arrows) were found but they can be seen more frequently in picture b) and c), dark dots in the picture d) are probably artefacts*

Even though the aluminium with high purity (1050 H24 Al - 99.5 wt%) was used for casting, eutectics appeared between primary dendrites. Unfortunately, the casted process which was used is not a closed thermodynamic system. The sources of the chemical diversity might be a graphite form, chemically treated surface of ceramic or a zinced iron wire.

The surface of the ceramic was chemically treated. However, the volume of compounds used for coating was extremely low. It is not likely that these compounds would lead to such an effect. It cannot be said what type of intermetallics it is, because the chemical composition is unknown.

Size of dendrites was a similar in all cases of thermal program. A volume of precipitated phases was almost identical in picture a), b) and d). It is important to say that the dark dots in 800 °C are artefacts. A higher concentration of micro-shrinkages was noticed in the picture b).

The picture c) shows the structure of aluminium in the vicinity of ceramic. The volume of precipitation is higher noticeably compared to a previous picture. Most probably this is caused by a higher heat capacity of ceramic and by its low thermal conductivity. The heat absorbed in the ceramic during a heating made the process of solidification slower in the surrounding of ceramic then in the distanced parts.

720 °C, 30 min, insulation C

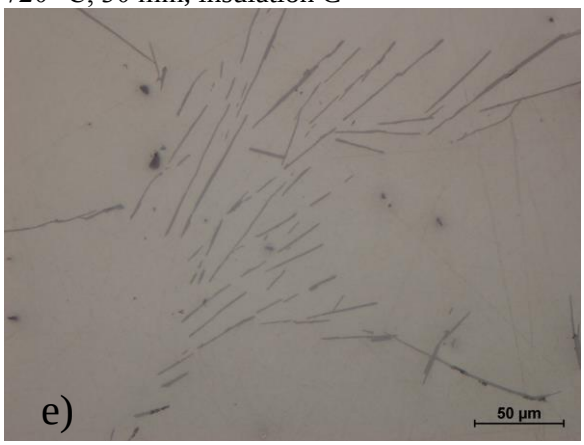


*Picture 47: Script like structure of the intermetallic phases*

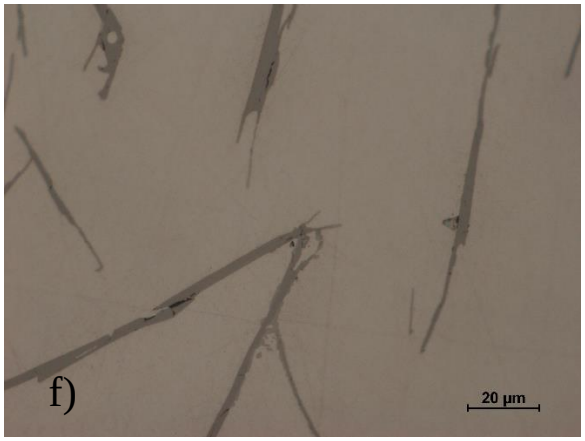


*Picture 48: The needle like shape of phases is similar to a shape of Si in silumins, however the real composition is probably different*

The shape of the phases is similar to Si needles formed in silumins. However, the existence of such phase is hardly possible.

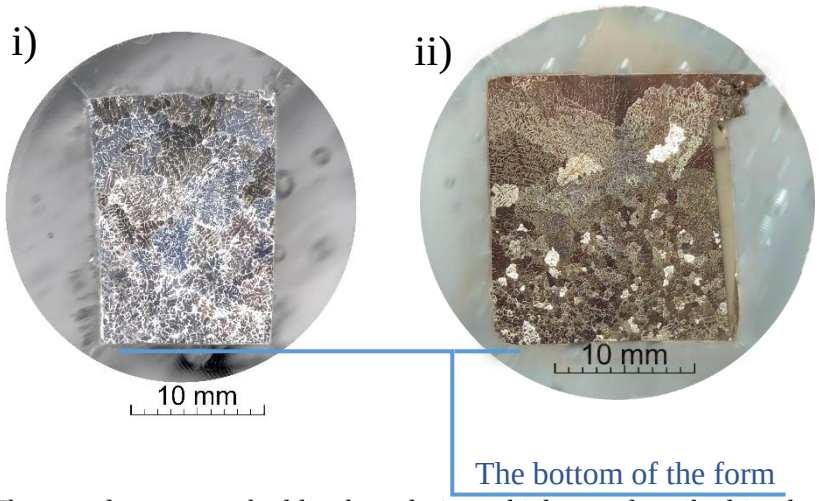


*Picture 49, 50: (i, ii) Macroscopic structure after etching, both samples were prepared by 720 °C, sample ii) was prepared from material after the ballistic test, grain size heterogeneity is visible, it is probably caused by the thermal gradient in form during the solidification, the orientation of pictures to the form is described by blue line*

The samples were etched by the solution which was described in chapter 4.5.1. Image ii) has a better contrast because it was etched for a longer time. The grain diversity is most probably caused by the thermal gradient during solidification. The aluminium on the bottom was cooled faster than the upper parts of the cast.

The effect of the ceramics on the grain size in the joint of alumina will be studied in the future.

### 4.4.2 Electron microscopy

Etched sample: 720 °C, 30 min, shot, interface

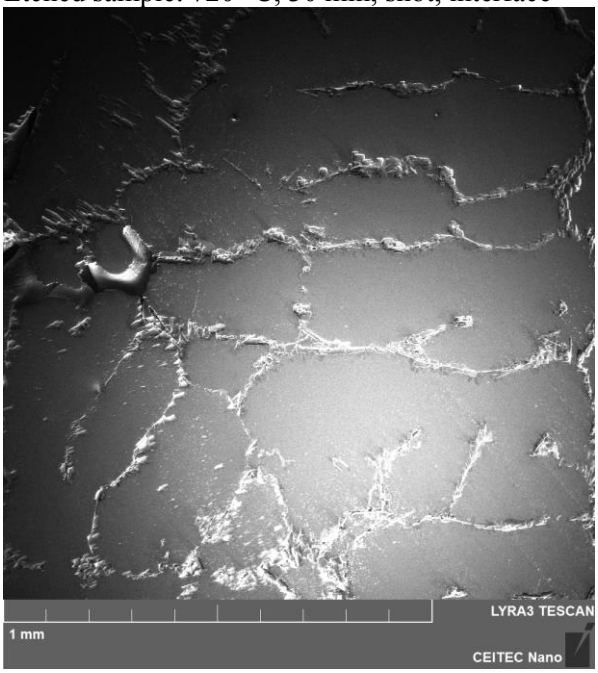


*Picture 51: BE shows a difference in contrast between matrix and vicinity of the phases*

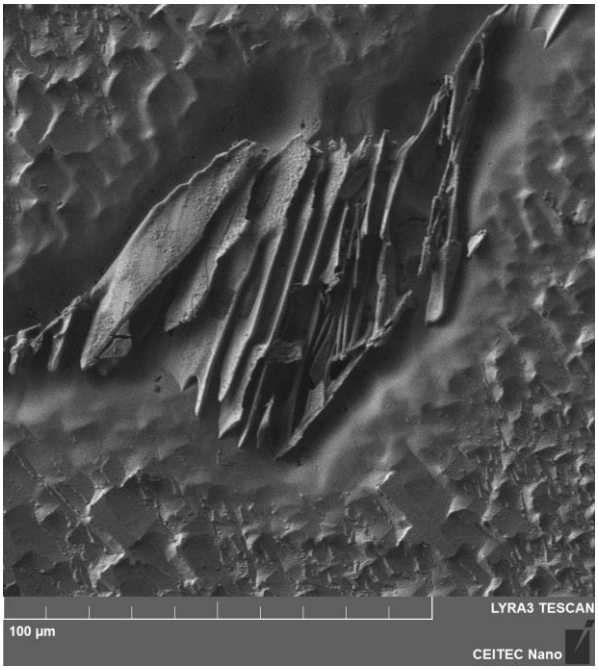


*Picture 52: SE, the vicinity of the eutectic was etched much easily then the phase itself*

Contrast between edge of dendrites and matrix was find by BE (Picture 51). That indicate an existence of a micro-segregation process.

The phase has a higher resistance against etching solution as it is shown in Picture 52. The composition of intermetallics is not known yet. One of the options is that they are formed by oxides, however this will be proved or disproved in subsequent research.

The full metallographic analysis was not aim of this work, however the preliminary results demonstrated unusual microstructure. The reason is non-conventional approach, when the aluminium with a high purity is prepared by non-standard conditions for aluminium alloys. High purity aluminium is unsuitable conventional for casting for its high temperature of melt and low casting properties.

Nevertheless, this material was used for its high plasticity which is important when the material is loaded in dynamic way.

# 5 CONCLUSIONS

Experimental part of the thesis was focused on finding the optimal temperature conditions for current alumina/aluminium composite. These conditions include the temperature transfer, the maximal temperature and the time of dwell time. The task was to increase an energetic efficiency without decrease of quality of the composite. The temperature was changed from 900 °C to 680 °C. Temperature 720 °C with dwell time 30 minutes showed to be suitable since the quality of cast was similar or better than at highest temperatures. However, another parameters such heating rate , dwell time and heat transfer plays similarly important role as the temperature.

Verification quality of alumina/aluminium interface prepared at 720 °C with dwell time 30 min was done by the ballistic test. The composite was tested according to the NATO standard 2280 and the fracture mechanism of interface was subjected to analysis. The results indicates a good properties of the interface, when cracks we observed in ceramic part and cavities in aluminium. No significant damage of the alumina/aluminium interface was observed.

Modified four-point bending test was used to verify strength of alumina/aluminium interface. This test was not successful in the measuring of the adhesion energy, but we can conclude that measured values dependent on quality of the aluminium itself. The possible reason is that the interface had a higher fracture toughness than the aluminium itself in the slow mode of loading.

Microstructure analysis was prepared to receive an additional feedback from the casting process. This test however revealed unexpected structures in the aluminium. The eutectoid phases occurred on the border of primary dendrites. It is likely that the phases formed from oxides from aluminium surface, on regard to the origin composition of aluminium input. The real composition is however unknown at this moment and need to be further investigated.

# LITERATURE


[1] ODANOVIĆ, Zoran a Biljana BOBIĆ. Ballistic protection efficiency of composite ceramics/metal armours. *ВОЈНОТЕХНИЧКИ ИНСТИТУТ* [online]. Београд, Србија: ВОЈНОТЕХНИЧКИ ИНСТИТУТ, 2003, 3/3/2003, **LIII**(3), 30-38 [cit. 2019-05-24]. Dostupné z: http://www.vti.mod.gov.rs/ntp/rad2003/3-03/odan/odan.pdf.

[2] *Lightweight ballistic composites: military and law-enforcement applications*. 2nd edition. Waltham, MA: Elsevier, 2016. ISBN 978-008-1004-067.

[3] DAVID, N. V., X.-L. GAO a J. Q. ZHENG. Ballistic Resistant Body Armor: Contemporary and Prospective Materials and Related Protection Mechanisms. *Applied Mechanics Reviews* [online]. 2009, **62**(5), 1-20 [cit. 2019-05-18]. DOI: 10.1115/1.3124644. ISSN 00036900. Dostupné z: http://AppliedMechanicsReviews.asmedigitalcollection.asme.org/article.aspx?articleid=1399404

[4] NOVÁČEK, Vojtěch. Vývoj hi-tech kompozitních sendvičů pro balistickou ochranu. Prague, 2013. Bacalar thesis. Czech technical university in Prague, Faculty of mechanical engeneering, Department of material science and engeneering. Vedoucí práce Zdeňka Jeníková..

[5] LAUSUND, Kristian. *Adhesion between ceramic and composite materials for use in lightweight ballistic armour*. OSLO, 2014. Master's Thesis. Universitet i Oslo, Faculty of Mathematics and Natural Sciences. Dostupné z: https://www.duo.uio.no/bitstream/handle/10852/40722/1/Adhesion-between-ceramic-and-compostie-materials-for-use-in-lightweight-ballistic-armour.pdf

[6] AKELLA, Kiran a Niranjan K. NAIK. Composite Armour: A Review. *Journal of the Indian Institute of Science* [online]. India: Journal of the Indian Institute o 312 f Science, 2015, July 2015, **Jul.–Sep. 2015**(VOL 95:3), 297-313 [cit. 2019-05-18]. ISSN 0970-4140. Dostupné z: https://www.researchgate.net/publication/283735712_Composite_armour_-_A_review?enrichId=rgreq-95a42d62f9a9a0a218217a268a700c7f-XXX&enrichSource=Y292ZXJQYWdlOzI4MzczNTcxMjtBUzozNjU4ODA1NjQzMDU5MjFAMTQ2NDI0NDEzMjI0OQ%3D%3D&el=1_x_2&_esc=publicationCoverPdf

[7] DOMNICH, Vladislav, Sara REYNAUD, Richard HABER a Manish CHHOWALLA. Boron Carbide: Structure, Properties, and Stability under Stress. Journal of the American Ceramic Society [online]. 2011, 94(11), 3605-3628 [cit. 2017-04-24]. DOI: 10.1111/j.1551-2916.2011.04865.x. ISSN 00027820. Dostupné z: http://doi.wiley.com/10.1111/j.1551-2916.2011.04865.x

[8] DRDLIK, Daniel, Jakub ROLECEK, Katarina DRDLIKOVA a David SALAMON. Restraining of calcium contamination in near-net shape alumina ceramics during slip casting. *International Journal of Applied Ceramic Technology* [online]. 2018, **15**(6), 1559-1566 [cit. 2019-05-19]. DOI: 10.1111/ijac.13042. ISSN 1546542X. Dostupné z: http://doi.wiley.com/10.1111/ijac.13042

[9] CARTER, C. Barry a M. Grant NORTON. *Ceramic materials: science and engineering*. 2nd ed. New York: Springer, c2013. ISBN 978-1-4614-3522-8.

[10] WADLEY, H.N.G., M.R. O'MASTA, K.P. DHARMASENA, B.G. COMPTON, E.A. GAMBLE a F.W. ZOK. Effect of core topology on projectile penetration in hybrid aluminum/alumina sandwich structures. *International Journal of Impact Engineering* [online]. 2013, **62**(December), 99-113 [cit. 2019-05-18]. DOI: 10.1016/j.ijimpeng.2013.05.008. ISSN 0734743X. Dostupné z: https://linkinghub.elsevier.com/retrieve/pii/S0734743X13001140

[11] Pressure Die Casting. In: *Download centre* [online]. Wiehl, Germany: © 2019 Kind & Co. Edelstahlwerk, GmbH & Co., s. 1-12 [cit. 2019-05-18]. Dostupné z: http://www.kind-co.de/en/download-centre.html?tx_kcdownloads_kcdownloads%5Bfile%5D=326&tx_kcdownloads_kcdownloads%5Baction%5D=download&tx_kcdownloads_kcdownloads%5Bcontroller%5D=Download&tx_kcdownloads_kcdownloads%5Bformat%5D=download&cHash=c1ea2d98c806f332e5a1fba5b47c3d79

[12] SCHULDIES, J.J. a R. NAGESWARAN. Ceramic matrix composites for ballistic protection of vehicles and personnel. *Blast Protection of Civil Infrastructures and Vehicles Using Composites* [online]. Elsevier, 2010, 2010, **2010**(7), 235-243 [cit. 2019-05-18]. DOI: 10.1533/9781845698034.2.235. ISBN 9781845693992. Dostupné z: https://linkinghub.elsevier.com/retrieve/pii/B978184569399250007X

[13] ASENOV, St., L. LAKOV a Kr. TONCHEVA. PROMISING CERAMIC MATERIALS FOR BALLISTIC PROTECTION. *Journal of Chemical Technology and Metallurgy* [online]. Bulgaria: Institute of Metal Science Equipment and Technologies"Acad. A. Balevski" with Hydro-& Aero Dynamic Center, Bulgarian Academy of Sciences, 2013, 2013, **48**(2), 190-195 [cit. 2019-05-18]. Dostupné z: http://dl.uctm.edu/journal/node/j2013-2/12-Asenov_Lakov_Toncheva-190-195.pdf

[14] Ceramic Material Properties 1. In: *TOP SEIKO Co.,Ltd.* [online]. Nagahama City, Shiga Pref., 526-0105 Japan: © TOP SEIKO Co. [cit. 2019-05-18]. Dostupné z: https://top-seiko.com/guide/graph/

[15] AZoM. Silicon Carbide (SiC) Properties and Applications. *AZO materials* [online]. 2001, Feb 5 2001, **2001**(Feb), 1-2 [cit. 2019-05-18]. Dostupné z: https://www.azom.com/article.aspx?ArticleID=42

[16] Sax, N.I. Dangerous Properties of Industrial Materials. 6th ed. New York, NY: Van Nostrand Reinhold, 1984., p. 2398

[17] B. SMETANA, M. TKADLEČKOVÁ, et al. DETERMINATION OF SOLIDUS AND LIQUIDUS TEMPERATURES FOR S34MnV STEEL GRADE BY THERMAL ANALYSIS AND CALCULATIONS. *Izvorni znanstveni rad* [online]. METALURGIJA, 2014, 2014, **53**(3), 295-298 [cit. 2019-05-18]. ISSN 0543-5846. Dostupné z: https://hrcak.srce.hr/file/176677

[18] ALUMINIUMS Alloys: Pure Aluminium 1050. *Sabater fundimol* [online]. Alicante, Spain: © 2004-2019 Fundiciones Sabater. S.L., , 16, 17 [cit. 2019-05-22]. Dostupné z: http://www.sabater-fundimol.com/customers/resources/pdf/sabater-fundimol_catalog_p16-17.pdf

[19] Mechanické a fyzikální vlastnosti hliníkových slitin: Hliníkové profily na míru. *AluNet* [online]. Pardubice, Czech Republic: ALUNET.cz © 2019, 2019 [cit. 2019-05-18]. Dostupné z: http://www.alunet.cz/pouzito

[20] Armox® 500T: High hardness armor with extrordinary toughness properties. *SSAB* [online]. Stockholm, SWEDEN: SSAB Copyright 2019, 2019 [cit. 2019-05-18]. Dostupné z: https://www.ssab.com/products/brands/armox/armox-500t?accordion=downloads

[21] SECURE 500_EN. In: *Publications* [online]. SECURE 500_EN. Duisburg, Gernany: thyssenkrupp Steel Europe ©, 2018, SECURE 500_EN, s. 1-4 [cit. 2019-05-18]. Dostupné z: https://www.thyssenkrupp-steel.com/media/content_1/publikationen/grobblech_migration/secure/werkstoffblaetter_4/secure_500_wbl_1943_englisch.pdf

[22] Advanced Alumina Materials: Manufacturing Processes. In: *CoorsTek* [online]. USA: © CoorsTek, 2016, 2016 [cit. 2019-05-19]. Dostupné z: https://www.coorstek.com/english/materials/technical-ceramics/alumina/

[23] Ballistic Performance of Titanium Alloys: Ti-6Al-4V Versus Russian Titanium. *Aberdeen Proving Ground* [online]. Aberdeen Proving Ground, 2018, February 2004, **2004**(February), 1-19 [cit. 2019-05-18]. Dostupné z: https://apps.dtic.mil/dtic/tr/fulltext/u2/a420984.pdf

[24] AUERKARI, Pertti. Mechanical and physical properties of engineering alumina ceramics. *Valtion teknillinen tutkimuskeskus* [online]. Technological research of Finland: https://www.vtt.fi/inf/pdf/tiedotteet/1996/T1792.pdf, 1996, 1996, **1996**, 1-26 [cit. 2019-05-18]. ISSN 1235-0605. Dostupné z: https://www.vtt.fi/inf/pdf/tiedotteet/1996/T1792.pdf

[25] Crystal structure of the parent structure of ruby. In: *Chemical Structure* [online]. Vesta [cit. 2019-05-18]. Dostupné z: https://chemicalstructure.net/portfolio/ruby/

[26] NIEDZINSKI, Michael. Advanced Aluminum Armor Alloys. *Light Metal Age* [online]. South San Francisco, USA: Copyright © Light Metal Age, 2019, December 19, 2016 [cit. 2019-05-18]. Dostupné z: https://www.lightmetalage.com/news/industry-news/flat-rolled-sheet/article-advanced-aluminum-armor-alloys/

[27] Unmatched protection with ArmX® solutions. *Arconic* [online]. Washington, D.C., USA: Copyright © 2019 Arconic, 2019, 2001, **2001**, 1-2 [cit. 2019-05-18]. Dostupné z: https://www.arconic.com/defense/catalog/armx_data_sheet.pdf

[28] CUI, Chunxiang, BaoMin HU, Lichen ZHAO a Shuangjin LIU. Titanium alloy production technology, market prospects and industry development. Elsevier Ltd. [online]. Elsevier, 2011, 32(3), 1-9 [cit. 2019-05-18]. DOI: 10.1016/j.matdes.2010.09.011. ISSN 02613069. Dostupné z: https://www.researchgate.net/publication/251540213_Titanium_alloy_production_technology_market_prospects_and_industry_development?enrichId=rgreq-52c5a6faef59b073bb127029497f2f7d-XXX&enrichSource=Y292ZXJQYWdlOzI1MTU0MDIxMztBUzo1Njg3NjgzNTk1NTA5NzZAMTUxMjYxNjM1MjQ4NA%3D%3D&el=1_x_2&_esc=publicationCoverPdf

[29] Potential Application of Titanium Alloys in Armor System [online]. TITANIUM EUROPE, 2019, 28. 9. 2006, 2006(28. 9.), 1-21 [cit. 2019-05-18]. Dostupné z: https://titanium.org/resource/resmgr/.../GOOCHWilliam_2011.pdf

[30] NIJ STANDARD 0108.01. *Ballistic Resistant Protective Materials*. September 1985. USA: U.S. Department of Justice National Institute of Justice, 1985.

[31] NATO AEP-55 STANAG 4569. *PROTECTION LEVELS FOR OCCUPANTS OF ARMOURED VEHICLES*. Brussels, Belgium: NATO STANDARDIZATION AGENCY AGENCE OTAN DE NoRMALISATION, 2012.

[32] NATO STANAG 2280. *TEST PROCEDURES AND CLASSIFICATION OF THE EFFECTS OF WEAPONS ON STRUCTURES*. EDITION A. Brussels, Belgium: NATO STANDARDIZATION AGENCY AGENCE OTAN DE NoRMALISATION, 2016.

[33] Experimental identification of adhesive properties between epoxy and glass. *ResearGate* [online]. Belgrade, Serbie: M.Sc. in mechanical engineering, University of Belgrade, 2008, 15 May 2014, **2008**(Januar), 1-155 [cit. 2019-05-18]. Dostupné z: https://www.researchgate.net/publication/37454421_Experimental_identification_of_adhesive_properties_between_epoxy_and_glass

[34] LACOMBE, Robert. *Adhesion measurement methods: theory and practice*. Boca Raton, FL: Taylor & Francis Group, 2006. ISBN 978-0824753610.

[35] P. 0., CHARALAMBIDES, J., LUND, A. 0., EVANS, R. iVI., MCMEEKING,A Test Specimen for Determining the Fracture Resistance of Bimaterial Interfaces. *ASME* [online]. USA: © ASME, 2019, MARCH 1989, **56**(82), 1-6 [cit. 2019-05-18]. Dostupné z: http://appliedmechanics.asmedigitalcollection.asme.org/journal.aspx

[36] Chao-Yu Lee. METAL/CERAMIC INTERFACE ENGINEERING - ADHESION STRENGTH MEASUREMENT BETWEEN DIELECTRIC CERAMIC AND ELECTRODE METAL. Mechanics [physics.med-ph]. Université Joseph-Fourier - Grenoble I; National Taiwan University, Taipei (Rep. of China), 2007. English

[37] SUANSUWAN, N. a M.V. SWAIN. Adhesion of porcelain to titanium and a titanium alloy. *Journal of Dentistry* [online]. 2003, **31**(7), 509-518 [cit. 2019-05-18]. DOI: 10.1016/S0300-5712(03)00071-X. ISSN 03005712. Dostupné z: https://linkinghub.elsevier.com/retrieve/pii/S030057120300071X

[38] DRDLIK, Daniel, Jakub ROLECEK, Katarina DRDLIKOVA a David SALAMON. Restraining of calcium contamination in near-net shape alumina ceramics during slip casting. *International Journal of Applied Ceramic Technology* [online]. 2018, **15**(6), 1559-1566 [cit. 2019-05-18]. DOI: 10.1111/ijac.13042. ISSN 1546542X. Dostupné z: http://doi.wiley.com/10.1111/ijac.13042

[39] POWERFIX® Multifunktionsöl/ Silikon- / PTFE-Spray. In: *Discounto* [online]. Germany: Copyright © DISCOUNTO GmbH 2019, 2019, 13.05.2017 [cit. 2019-05-18]. Dostupné z: https://www.discounto.de/Angebot/POWERFIX-Multifunktionsoel-Silikon-PTFE-Spray-2043884/

[40] LI, Ming-Yuan, Bai-Qing XIONG, Guo-Jun WANG, You-Zhi TONG, Xi-Wu LI, Shu-Hui HUANG, Zhi-Hui LI a Yong-An ZHANG. Fracture mechanism of a laminated aluminum alloy plate during ballistic impact. *Rare Metals* [online]. Berlin: © 2018 Springer Nature Switzerland, 2017, **36**(9), 737-745 [cit. 2019-05-23]. DOI: 10.1007/s12598-015-0684-1. ISSN 1001-0521. Dostupné z: http://link.springer.com/10.1007/s12598-015-0684-1

[41] M. Zhe , O. Dezellus , G. Parry , M. Braccini & J. C. Viala (2012) Modified 4-Point Bending Test for Adhesion Measurement at the Interface of Iron Coated with Aluminum Casting Alloy, Journal of Adhesion Science and Technology, 26:1-3, 1-17

[42] Properties and Characteristics of Silicon Carbide. In: Poco Graphite [online]. USA: ©1997 - 2017 Poco Graphite, 2002, 2002 [cit. 2019-05-19]. Dostupné z: http://www.poco.com/Portals/0/Properties.and.Characteristics.of.Silicon.Carbide.pdf.

# ABBREVIATIONS AND SYMBOLS

## Abbreviations

| | |
|---|---|
| AFV | Armoured fighting vehicle |
| α / hcp | Hexagonal close packed lattice |
| BSE | Backscattered electrons |
| HBW | Hardness by Brinell - wolfram indenter |
| HV | Hardness by Vickers |
| KE | Kinetic energy |
| LAV | Light armoured vehicles |
| MIG | Metal inert gas welding |
| NATO | North Atlantic Treaty Organization |
| NIJ | National Institute of Justice |
| PEG | Polyethylene glycol |
| PVA | Polyvinyl alcohol |
| SEM | Scanning electron microscope |
| SE | Secondary electron microscopy |
| STANAG | STANdardization Agreement |
| RHA | Rolled homogenous armour steel |
| WIG | Wolfram inert gas welding |
| 4PBT | Four-point beam bending test |

## Symbols

| Symbol | Units | Meaning |
|---|---|---|
| E | [J] | Energy of adhesion |
| h | [mm] | Thickness |
| $P_{cr}$ | [MPa] | Critical load |
| r | [mm] | Radius |
| S | [$cm^2$] | Surface |
| V | [$cm^3$] | Volume |
| $V_{200}$ | [$m \cdot s^{-1}$] | Velocity at 200 m |
| $\bar{m}$ | [kg] | Average mass |
| $\bar{h}$ | [cm] | Average weight |
| ρ | [$g \cdot cm^{-3}$] | weight density |
| # | [$grains \cdot cm^{-2}$] | grit size |
| ΔT | [°C] | Thermal change |

# APPENDIX

## I. Ballistic standards - kinetic threats

**NIJ standard – 0108.01**

**Table 1. *Test Summary***

| Test Variables | | Performance Requirements | | | | |
|---|---|---|---|---|---|---|
| Armor Type | Test Ammunition | Nominal Bullet Mass | Suggested Barrel Length | Required Bullet Velocity | Required Hits Per Armor Specimen | Permitted Penetrations |
| I | 22 LRHV<br>Lead | 2.6 g<br>40 gr | 15 to 16.5 cm<br>6 to 6.5 in | 320 ± 12 m/s<br>1050 ± 40 ft/s | 5 | 0 |
| | 38 Special<br>RN Lead | 10.2 g<br>158 gr | 15 to 16.5 cm<br>6 to 6.5 in | 259 ± 15 m/s<br>850 ± 50 ft/s | 5 | 0 |
| II-A | 357 Magnum<br>JSP | 10.2 g<br>158 gr | 10 to 12 cm<br>4 to 4.75 in | 381 ± 15 m/s<br>1250 ± 50 ft/s | 5 | 0 |
| | 9 mm<br>FMJ | 8.0 g<br>124 gr | 10 to 12 cm<br>4 to 4.75 in | 332 ± 12 m/s<br>1090 ± 40 ft/s | 5 | 0 |
| II | 357 Magnum<br>JSP | 10.2 g<br>158 gr | 15 to 16.5 cm<br>6 to 6.5 in | 425 ± 15 m/s<br>1395 ± 50 ft/s | 5 | 0 |
| | 9 mm<br>FMJ | 8.0 g<br>124 gr | 10 to 12 cm<br>4 to 4.75 in | 358 ± 12 m/s<br>1175 ± 40 ft/s | 5 | 0 |
| III-A | 44 Magnum<br>Lead SWC Gas Checked | 15.55 g<br>240 gr | 14 to 16 cm<br>5.5 to 6.25 in | 426 ± 15 m/s<br>1400 ± 50 ft/s | 5 | 0 |
| | | | | | 5 | 0 |
| | 9 mm<br>FMJ | 8.0 g<br>124 gr | 24 to 26 cm<br>9.5 to 10.25 in | 426 ± 15 m/s<br>1400 ± 50 ft/s | | |
| III | 7.62 mm<br>308 Winchester<br>FMJ | 9.7 g<br>150 gr | 56 cm<br>22 in | 838 ± 15 m/s<br>2750 ± 50 ft/s | 5 | 0 |
| IV | 30-06<br>AP | 10.8 g<br>166 gr | 56 cm<br>22 in | 868 ± 15 m/s<br>2850 ± 50 ft/s | 1 | 0 |
| Special Requirement (see sec. 2.2.7)* | * | * | * | * | * | * |

* These items must be specified by the user. All of the items must be specified.

Abbreviations: AP - Armor Piercing
FMJ - Full Metal Jacket
JSP - Jacketed Soft Point
LRHV - Long Rifle High Velocity
RN - Round Nose
SWC - Semi-Wadcutter

*Table 8: Performance Requirements NIJ Standard-0108.01 [30]*

**NATO AEP-55 STANAG 4569**

KE PROTECTION LEVELS FOR OCCUPANTS OF ARMOURED VEHICLES

| Level | KE-Threat | Reference – Artillery – Threat |
|---|---|---|
| 6 | Weapon: Automatic Cannon, 30 mm<br>Ammunition: APFSDS and AP<br>Distance: 500 m<br>Angle: frontal arc to centreline: ± 30° sides included; elevation 0° | Artillery 155 mm<br>Estimated range of burst: 10 m<br>Azimuth 360°<br>Elevation: 0 - 90° |
| 5 | Weapon: Automatic Cannon, 25 mm<br>Ammunition: APDS and APFSDS<br>Distance: 500 m<br>Angle: frontal arc to centreline: ± 30° sides included; elevation 0° | Artillery 155 mm<br>Estimated range of burst: 25 m<br>Azimuth 360°<br>Elevation: 0 - 90° |
| 4 | Weapon: Heavy Machine Gun, 14.5 mm<br>Ammunition: AP<br>Distance: 200 m<br>Angle: azimuth 360°; elevation 0° | Artillery 155 mm<br>Estimated range of burst: 25 m<br>Azimuth 360°<br>Elevation: 0 - 90° |
| 3 | Weapon: Machine Gun and Sniper rifles, 7.62 mm<br>Ammunition: AP tungsten carbide and AP hard steel core<br>Distance: 30 m<br>Angle: azimuth 360°; elevation 0-30° | Artillery 155 mm<br>Estimated range of burst: 60 m<br>Azimuth 360°<br>Elevation: 0° – 30° |
| 2 | Weapon: Assault rifles, 7.62 mm<br>Ammunition: AP steel core<br>Distance: 30 m<br>Angle: azimuth 360°; elevation 0-30° | Artillery 155 mm<br>Estimated range of burst: 80 m<br>Azimuth 360°<br>Elevation: 0° – 22° |
| 1 | Weapon: Assault rifles:7.62 and 5.56 mm<br>Ammunition: Ball<br>Distance: 30 m<br>Angle: azimuth 360°; elevation 0-30° | Artillery 155 mm<br>Estimated range of burst: 100 m<br>Azimuth 360°<br>Elevation: 0° – 18° |

As notification of the protection level is advised to use the first character of the threat followed by the protection level (e.g. K2).

*Table 9: Performance Requirements NATO AEP-55 STANAG 4569 [31]*

**NATO STANAG 2280**

| | | Type | Remarks |
|---|---|---|---|
| A5 | 30 mm APDS<br>(Range 500 m) | • 30 x 170 mm L14A2 / A3<br>(Rarden / Bushmaster II) | $V_0$ = 1170 m/s, m = 300 g<br>Tungsten penetrator,<br>$V_{500}$ = 1100 m/s (*) |
| | | • 30 x 165 mm<br>(2A42 gun, e.g. BMP-2) | $V_0$ = 1120 m/s, m = 400 g<br>Tungsten core 222 g,<br>$V_{500}$ = 1030 m/s (*) |
| | | • 30 x 173 mm Oerlikon Mk 30<br>(Bushmaster II / Mauser Mk 30) | $V_0$ = 1225 m/s, m = 225 g<br>Tungsten penetrator,<br>$V_{500}$ = 1135 m/s (*) |
| A4 | 12.7 - 14.5 mm AP<br>(Range 200 m) | • 14.5 mm x 114 API B32<br>• 12.7 mm x 108 API B32<br>• 12.7 mm x 99 API M8 | $V_{200}$ = 900 m/s (**), m = 64 g<br>$V_{200}$ = 760 m/s (**), m = 48 g<br>$V_{200}$ = 800 m/s (**), m = 43 g |
| A3 | 7.62 mm AP WC<br>(Range 30 m) | • 7.62 mm x 51 AP (WC) M993<br>• 7.62 mm x 54R API B32 (***) | Tungsten core<br>$V_0$ = 893 m/s, m = 8.3 g<br>$V_0$ = 874 m/s, m = 10.4 g |
| A2 | 5.56 - 7.62 mm AP<br>(Range 30 m) | • 7.62 mm x 51 AP M61<br>• 7.62 mm x 39 AP 7N23<br>• 7.62 mm x 51 Lead free NM 231<br>• 5.56 mm x 45 Lead free NM 229 | $V_0$ = 838 m/s, m = 9.8 g<br>$V_0$ = 740 m/s, m = 7.9 g<br>$V_0$ = 830 m/s, m = 9.0 g<br>$V_0$ = 930 m/s, m = 4.0 g |
| A1 | 5.56 - 7.62 mm Ball<br>(Range 30 m) | • 7.62 mm x 51 M80<br>• 7.62 mm x 39 57N231<br>• 5.56 mm x 45 M193<br>• 5.56 mm x 45 SS109 | Lead core, 854 m/s, m = 9.3 g<br>Steel core, 725 m/s, m = 8.0 g<br>Lead core, 975 m/s, m = 3.6 g<br>Steel tip, 930 m/s, m = 4.0 g |

(*) $V_{500}$ data not available at the time of writing. Estimates assumes penetrator diameter 15 mm

(**) Calculated from the following muzzle velocities: $V_0$ = 976 m/s (14.5 mm), $V_0$ = 840 m/s (12.7 mm x 108), $V_0$ = 880 m/s (12.7 mm x 99)

(***) This projectile does not have a Tungsten core, but is included in class A3 in accordance with STANAG 4569

*Table 10: Performance Requirements NATO STANAG 2280 [31]*

## II. Insulation grades

In the following chapters insulation will be described by the insulation grade. This is a brief description of insulation grades. Four grades were defined in total. The lowest grade C describes the situation when no insulation was used. B, A, A+ grades describes a design in which the insulation was placed inside the furnace.

Two materials were used as an insulation, but most often it was 1 mm thick graphite felt (thermal conductivity, k ~ 0, 2 $Wm^{-1}K^{-1}$). The second material was the 40 mm thick WDS board (thermal conductivity, k ~ 0,02 $Wm^{-1}K^{-1}$). The board from WDS was cut and it was used as a "cap".

Graphite felt

WDS board

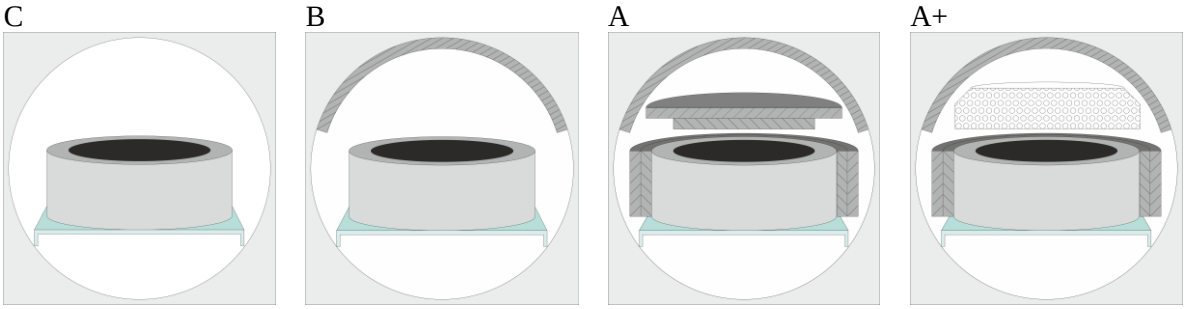


*Picture 53: A schematic illustration of the insulation composition in the furnace, C – only graphite form without any insulation is placed in furnace, B – basic 1 mm graphite felt cover, A + 2 mil cap + 1 mm cover, A+ –2 x 1 mm thick graphite felt wrapped around the form + WDS cap + basic cover*

III. Samples selection and preparation

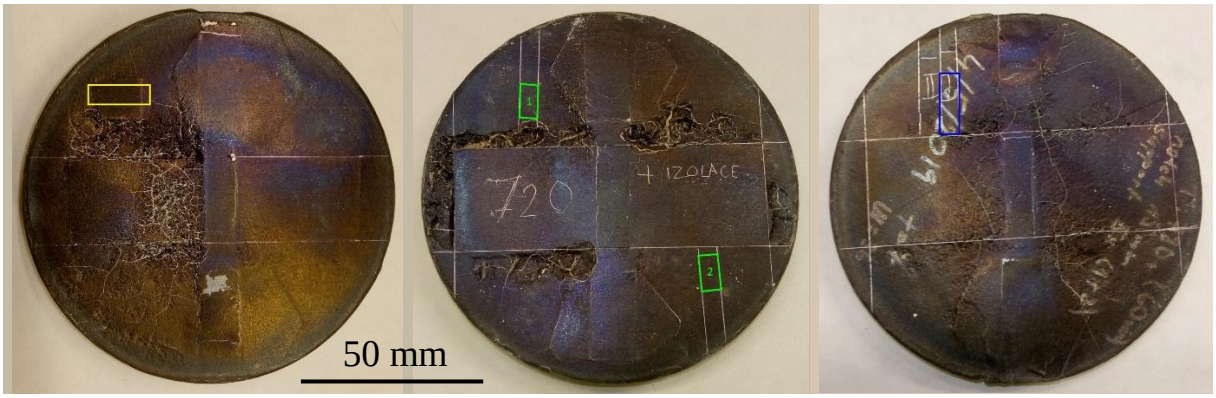


*Picture 54: 720 °C, 30 min, interface non-shot, insulation B*

*Picture 55: 720 °C, 30 min, insulation A*

*Picture 56: 720 °C, 60 min, insulation A+*

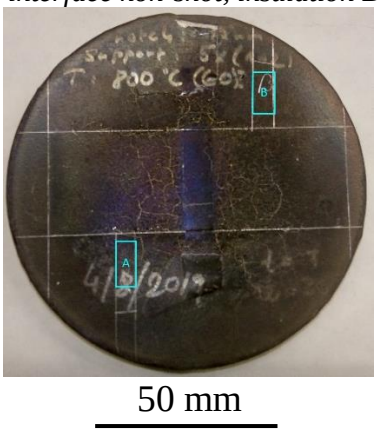


*Picture 57: 800 °C, 30 min*

| | Abrasive size / type | Suspension / Lubricant | Rpm | Time | Force |
|---|---|---|---|---|---|
| Grinding | | | | | |
| 1st Step | # 500 / SiC Paper | Water | 250 | 1 min | low |
| 2nd Step | # 800 / SiC Paper | Water | 250 | 1 min | low |
| 3rd Step | # 1200 / SiC Paper | Water | 250 | 1 min | low |
| 4th Step | # 2400 / SiC Paper | Water | 250 | 1 min | low |
| 5th Step | # 4000 / SiC Paper | Water | 250 | 2 min | low |
| Polishing | | | | | |
| 1st Step | 3 µm / Diamond | 3 µm paste / Ethanol | 125 | 4 min | very low |
| 2nd Step | 0.7 µm / Diamond | 0.7 µm / Ethanol | 125 | 10 min | very low |
| 3rd Step | 0.04 µm / Colloidal Silica | OP – S | 125 | 2 + 4 min | very low |
| 4th Step | 0.7 µm / Diamond | 0.7 µm / Ethanol | 125 | 10 min | very low |

*Table 11: Sample preparation, grinding and polishing process*

## IV. Four-point beam bending - specimens


*Picture 58 – 70: Specimens description, yellow areas shows imperfections in the body of aluminium, A – imperfection pinhead size, C – imperfection approximately 2 cm$^2$ 0.5 mm deep, F – imperfection approximately 2 cm$^2$ 0.5 mm deep*